Jestr

Journal of Engineering Science and Technology Review 17 (2) (2024) 77 - 96

Research Article

JOURNAL OF
Engineering Science and Technology Review

www.jestr.org

Application of Modified Flow Direction Algorithm for Network Reconfiguration with Distributed Generator Installation

K. Kalyan Kumar* and G. Nageswara Reddy

Department of Electrical & Electronics Engineering, YSR Engineering College of Yogi Vemana University, India

Received 13 December 2023; Accepted 27 February 2024

Abstract

This article used an improved version of the Flow Direction Algorithm (FDA) with acceleration coefficients named Modified Flow Direction Algorithm (MFDA) for simultaneous Optimal Network Reconfiguration (ONR) and Optimal Distribution Generation's (ODG) installation to reduce the Active Power Losses (APL), maximize the Voltage Profile (VP) and stability of the Distribution System (DS). FDA is motivated by the simulation of the direction of water flow into a drainage basin at a lower elevation area. The neighboring flow and its slope also affect the direction of the water flow; its slope was obtained using the D8 method. FDA has a low convergence rate, stuck with local optima. This article proposed acceleration coefficients to acquire the proper balance between exploration and exploitation, accelerate the global convergence rate, and avoid getting stuck with local optima. The efficiency of the MFDA is evaluated based on its performance on 16 standard benchmark functions and is also used to solve the simultaneous ONR and ODG installation. Two DSs consisting of 33 and 69 bus test systems are considered to solve the problem. There are three methodologies to reduce the APL and maximize the VP and stability: ONR, ODG, and simultaneous ONR and ODG installation. This article uses four case studies with different load levels to show the proposed method's reliability. The analysis shows a better way to minimize the power loss by solving simultaneous ONR and ODG installation rather than only optimizing reconfiguration or installation of DG. It has been discovered that the results achieved are superior to those produced using the ISCA, FWA, HSA, etc. So, the MFDA shown can be a potentially useful way to solve 16 standard benchmark functions and simultaneous ONR and ODG installation.

Keywords: Distribution System, Power Losses, Voltage Profile Improvement, Network Reconfiguration, Distributed Generation Installation, Mathematical Modeling, Flow Direction Algorithm, Modified Flow Direction Algorithm.

1. Introduction

The primary goal of today's electric power system is to consistently and economically meet consumer needs. This power system may be categorized into three sectors: generation, transmission, and distribution systems. Out of all the sectors, the DS is important in providing electricity to loads; distribution systems typically have "low voltage and high current levels" [1] and have high power loss and poor voltage profiles because of their structural and operational characteristics. Most studies have found that reducing the APL in DS is a significant goal. So, the most common approaches are ONR, ODG installation, and optimal Shunt Capacitors (SCs) installation to reduce the APL and maximize the VP and stability. However, most researchers focused on simultaneous ONR and ODG installation due to attractive and alternative solution methodologies to reduce the APL and maximize the VP and stability [2 - 3].

Network reconfiguration adjusts the network topology by exchanging switches open/closed status to obtain a radial configuration that reduces power losses and enhances voltage profile through meeting operational constraints. Most researchers have handled the challenges with network reconfiguration and proposed a variety of approaches to minimize the losses, and maximize the voltage profile and stability. So many researchers solved this challenge using novel meta-heuristic techniques like C. Wang and H. Z. Cheng used Plant Growth Simulation Algorithm (PGSA) [4], A. Y. Abdelaziz et al. used a modified Particle Swarm Optimization (PSO) [5], Y. K. Wu used an Ant Colony Algorithm (ACA) [6], R. Srinivasa Rao et al. used Harmony Search Algorithm (HAS) [7], A. Y. Abdelaziz et al. used Ant Colony Optimization (ACO) and HAS [8], J. A. Martín García and A. J. Gil Mena used a modified Teaching-Learning Based Optimization Algorithm (TLBO) [9], J. Torres et al. used a GA based on the edge window decoder (GA-EWD) [10], Y. Lakshmi Reddy et al. used Firefly Algorithm (FFA) [11], E. Azad-Farsani et al. used Particle Swarm Optimization (CPSO) and TLBO named as hybrid CPSO-TLBO [12], S. Teimourzadeh and K. Zare used Binary Group Search Optimization (BGSO) [13], R. Sedaghati et al. used Adaptive Modified Firefly Algorithm (AMFA) [14], M. Abdelaziz used Genetic Algorithm (GA) [15] with varying population size, R. Pegado et al. used Binary Particle Swarm Optimization (BPSO) [16], T. Tran The used Chaotic Stochastic Fractal Search Algorithm (CSFSA) [17], T. T. Nguyen et al. used Improved Coyote Optimization Algorithm (ICOA) [18], H. Hizarci et al. used Time-Varying Acceleration Coefficient Binary PSO (TVAC-BPSO) [19], M. Cikan and B. Kekezoglu used Equilibrium Optimizer (EO) [20] to solve optimal network reconfiguration.

Distributed generation resources are becoming more common as essential parts of the power system. Many benefits may be gained through DGs in the networks, including lower losses and enhanced voltage profiles. DG's

*E-mail address: kalyankumark13@gmail.com
ISSN: 1791-2377 © 2024 School of Science, DUTH. All rights reserved.
doi:10.25103/jestr.172.11

optimal position and sizing must be determined to maximize the benefits during the distribution system development. Therefore, it's essential to identify DG's suitable size and position in the DS without disturbing the present system architecture. Hence, DG installation is an essential problem in the DS. The DS's operators and researchers used many innovative meta-heuristic algorithms to solve this problem, such as Y. J. Jeon et al. used Hereford Ranch Algorithm (HRA) [21], E. Haesen et al. used Monte Carlo Simulations Algorithm (MCSA) [22], M. R. Alrashidi and M. F. Alhajri used an improved PSO [23], F. S. Abu-Mouti and M. E. El-Hawary used Artificial Bee Colony (ABC) [24], M. H. Moradi and M. Abedini used combined GA (GA)/ PSO names as GA/PSO [25], H. Doagou-Mojarrad et al. used Hybrid Evolutionary Algorithm (HEA) [26], M. M. Aman et al. used multi-objective Particle Swarm Optimization (PSO) [27], and Hybrid HPSO [28], A. El-Fergany used Backtracking Search Algorithm (BSA) [29], N. Kanwar et al. an improved TLBO [30], D. Rama Prabha and T. Jayabarathi used Invasive weed optimization (IWO) [31], E. S. Oda et al. used Flower Pollination Algorithm (FPA) [32], S. A. Chithra Devi et al. used Stud Krill herd Algorithm (SKHA) [33], U. Sultana et al. used Grey Wolf Optimizer (GWO) [34], H. Hamour et al. used Grasshopper Optimization Algorithm (GOA) [35], D. B. Prakash and C. Lakshminarayana used Whale Optimization Algorithm (WOA) [36], S. Kamel used Hybrid Gray Wolf Optimizer (HGWO) [37], J. Radosavljevic et al. used hybrid phasor PSO and gravitational search algorithm (HPPSOGSA) [38], G. Deb et al. used Spider Monkey Optimization (SMO) [39], A. Selim used improved version of Harris Hawks optimizer (IHHO & MOHHO) [40], K. H. Truong et al. used Quasi-Oppositional Chaotic Symbiotic Organisms Search (QOCSOS) [41], Z. Tan et al. used Swarm Moth Flame Optimization (SMFO) [42], M. G. Hemeida et al. used Manta Ray Foraging Optimization algorithm (MRFO) [44], K. S. Sambaiah and T. Jayabarathi used Salp Swarm Algorithm (SSA) [45], to solve the ODG installation problem.

All the above researchers focused only on optimizing network reconfiguration or DG installation. This paper focuses on simultaneous NR and DG installation through power loss as an objective function significantly contributing to technological advancement. Most recent works have combined network reconfiguration with DG installation to boost electrical distribution system efficiency. "In [46], the authors used the HAS to simultaneously handle network reconfiguration and DG installation while focusing exclusively on reducing power losses". Afterward, many scholars used many innovative meta-heuristic algorithms to solve this problem, like S. H. Mirhoseini et al. used the Improved Adaptive Imperialist Competitive Algorithm (IAICA) [47], T. T. Nguyen et al. used an Adaptive Cuckoo Search Algorithm (ACSA) [48], S. R. Tuladhar used Non-Dominated Sorting Particle Swarm Optimization (NSPSO) [49], A. Bayat used a "Uniform Voltage Distribution based constructive reconfiguration Algorithm" (UVDA) [50], M. Abd El-salam used a hybridization of GWO and PSO named as (GWO-PSO) [51], J. Siahbalaee et al. used Improved Shuffled Frog Leaping Algorithm (ISFLA) [52], A. Onlam et al. used a novel Adaptive ASFLA [53], U. Raut and S. Mishra used an Elitist–Jaya algorithm (IE-JAYA) [54], I. A. Quadri and S. Bhowmick used a hybridization of the TLBO and the HSA, it is named as CTLHSO) [55], T. T. The et al. used Symbiotic Organism Search (SOS) Algorithm [56], H. Teimourzadeh and B. Mohammadi-Ivatloo used a three-dimensional group search optimization (3D-GSO) [57], T. T. Tran et al. used a Stochastic Fractal Search (SFS) algorithm [58], K. S. Sambaiah and T. Jayabarathi used a SSA [59], U. Raut and S. Mishra used an Enhanced Sine–Cosine Algorithm (ESCA) [60], T. T. Nguyen used a Pathfinder Algorithm (PFA) [61], A. M. Shaheen et al. used an Improved EO Algorithm (IEOA) [62], T. Van Tran et al. used a new Quasi-Oppositional Chaotic Neural Network Algorithm (QOCNNA) [63], M. T. Nguyen Hoang et al. used a Quasi-Oppositional-Chaotic SOS (QOCSOS) Algorithm [64], T. T. Nguyen et al. used a Multi-Goal Function Based on Improved Moth Swarm Algorithm (MFA) [65], M. Ntombela et al. used a hybridization of the GA and the improved PSO (IPSO) named as (HGAIPSO) [66], and M. Shaheen et al. used a Modified Marine Predators Optimizer (MMPO) [67] to solve the simultaneous NR and DG installation problem.

Recently, a modern physics-based meta-heuristic algorithm, the Flow Direction Algorithm (FDA), was developed by Karami et al. [69]. The stochastic nature of the FDA gets trapped at local optimums and has a poor convergence rate. In response to these issues, our research suggests acceleration coefficients to boost the performance of the FDA. This modified version of the FDA effectively tackles the benchmark functions, and the MFDA deals with ONR, ODG installation, and simultaneous ONR and ODG installation. The analysis shows a better way to minimize the power loss by solving simultaneous ONR and ODG installation rather than only optimizing reconfiguration or installation of DG. It has been discovered that the outcomes achieved are superior to those produced outcomes using the ISCA, the FWA, the HSA, etc.

Table 1. Nomenclature

Abb	Desciption
APL	Active Power Losses
APLRI	Active Power Losses Reduction Index
C1 & C2	Acceleration Coefficients
DS	Distribution System
Is	Maximum Acceptable Current through S Line
iter	Iteration
Flow_Xnew	New Water Flow Position
Max_iter	Maximum no. of Iterations
Nbus	Number of Buses
Neighbor	Neighbor Water Flow Position
lb	Lower Bound
NDG	Total Number of DGs
OF	Objective Function
ODG	Optimal Distribution Generation
ONR	Optimal Network Reconfiguration
PDG	Active Power Supplied by DG
Ps	Real Power Flowing out of Bus S
Psub	Active Power Supplied by Substation
PL	Power Loss
PLs+1	Real Load Powers at Bus S+1
Qs	Reactive Power Flowing out of Bus S
QLs+1	Reactive Load Powers at Bus S+1
rand	Random Value with Uniform Distribution
randn	Random Value with Normal Distribution
RPL	Reactive Power Loss
RPLRI	Reactive Power Losses Reduction Index
Rs	Line Resistance
SCs	Shunt Capacitors
S0	Slope between the Current and Neighbor Water Flows
TPL	Total System Loss
$T_{PL,(DG)}$	Total APL in the Presence of DG
$T_{QL,(DG)}$	Total RPL in the Presence of DG
V	Velocity
Vmin	Lower Acceptable Voltages
Vmax	Upper Acceptable Voltages
VP	Voltage Profile
VPI	Voltage Profile Improvement
ub	Upper Bound
X_Best	Best Water Flow Position

X_Flow	Water Flow Position
Xrand	Random Position
Xs	Line Reactance
W	Nonlinear Weight with a Random Number between 0 and Infinity
β	Number of Neighbours
Δ	Neighbourhood Radius

2. Problem Formulation

The only way to enhance the effectiveness of the distribution system is to minimize power losses. Also, the main contribution made by this article is to plan for the best possible reconfiguration of the DS and installation of DG by taking the switches and tie switches status and the location and size of DG units. This article aims to reduce distribution system losses when operating under different load levels due to operational constraints. The formal mathematical statement of the problem is as follows:

$$\min OF=\min(TP_L) \quad (1)$$

where,
TP_L is the total system loss.

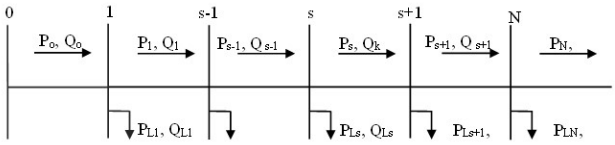

Fig. 1. Radial-feeder Single-line diagram.

The single-line diagram of radial-feeder may be seen in Figure 1 [68]. The recursive equations below have been supplied to determine the power flow [2, 3, and 68]. Power flow calculations can be done using the Newton-Raphson technique with the software tool MATPOWER [71].

$$P_{s+1}=P_s-P_{Ls+1}-R_{s,\,Ls+1}\bullet\frac{\left(P_s^2+Q_s^2\right)}{|V_s|^2} \quad (2)$$

$$Q_{s+1}=Q_s-Q_{Ls+1}-X_{s,\,Ls+1}\bullet\frac{\left(P_s^2+Q_s^2\right)}{|V_s|^2} \quad (3)$$

$$|V_{(s+1)}|^2=|V_s|^2+2\left(R_{s,\,(s+1)}\bullet P_s+X_{s\,(s+1)}\bullet Q_s\right)+\left(R_{s,\,(s+1)}^2+X_{s,\,(s+1)}^2\right)\frac{(P_s^2+Q_s^2)}{|V_s|^2} \quad (4)$$

"where P_s and Q_s are the real and reactive power flowing out of bus s, P_{Ls+1} and Q_{Ls+1} are the real and reactive load powers at bus s+1. The line section between buses s and s+1 has resistance $R_{s,\,s+1}$ and reactance $X_{s,\,s+1}$" [73].
The PL of the feeder is calculated by

$$P_L(s,\,s+1)=R_{s,\,Ls+1}\bullet\frac{\left(P_s^2+Q_s^2\right)}{|V_s|^2} \quad (5)$$

The total PL of the feeder is calculated by

$$TP_L=\sum_{s=0}^{n-1}P_L(s,\,s+1) \quad (6)$$

2.1 System Constraints

The outcomes acquired by the proposed technique would be subjected to equality and inequality constraints to identify the optimal outcomes of the problem.

Equality Constraints
The balance between power demand and supply is given by

$$TP_{sub}+\sum_{s=1}^{NDG}P_{DG,n}-\sum_{s=2}^{N_{bus}}PL_s-TPL_{DG}=0 \quad (7)$$

P_{sub} and P_{DG} are the active power supplied by substation and DG, respectively; P_{Ls} is the total active power demand at bus, $TP_{L,\,(DG)}$ is the total APL in the presence of DG, N_{bus} is the number of buses. N_{DG} is the total number of DGs.

Inequality Constraints
System constraints should be satisfied during the ONR, ODG, and simultaneous ONR and ODG installation. All system bus voltages must be maintained between lower and upper limits. Current in a branch cannot exceed its rated capacity in the system. Mathematically, these constraints are expressed as follows:

$$V_{min}\le V\le V_{max} \quad (8)$$

$$|I_s|\le I_{s,\,max} \quad (9)$$

where,
V_{min} and V_{max} are the lower and upper acceptable voltages for any bus in the system,
V_{min} is 0.9 and V_{max} is 1.05 (p.u.).
I_s is the s^{th} line current,
$I_{s,\,max}$ is the maximum acceptable current through the line.

DG Limits
A random selection is used to attain the DG size, normalized between the minimum and maximum operational limitations. The lower bound is 10%, and the upper bound is 60% of the total active power demand. These limits are derived as follows [3, 35].

$$0.1\times\sum_{s=2}^{N_{bus}}PL_s\le\sum_{s=1}^{NDG}P_{DG,s}\le 0.6\times\sum_{s=2}^{N_{bus}}PL_s \quad (10)$$

2.2 Performance Indices

The following assessment indices determine how well the suggested strategy works for reconfiguring and optimally integrating DG. Higher values indicate a more favorable influence on each index's distribution system.

APL Reduction Index (APLRI)

APLRI is determined from Eq. (11) [57].

$$APLRI\ (\%)=\frac{TP_L-TP_{L\,(NR+DG)}}{TP_L}\times 100 \quad (11)$$

TPL and TPL (NR+DG) are the total APL in cases 1 and 4.

RPL Reduction Index (RPLRI)
RPLRI is determined from Eq. (12) [57].

$$RPLRI\ (\%)=\frac{TQ_L-TQ_{L(NR+DG)}}{TQ_L}\times 100 \quad (12)$$

TQL and TQL (NR+DG) are the total RPL in cases 1 and 4.

Voltage Profile Improvement (VPI)
VPI is determined from Eq. (13) [57].

$$VPI\ (\%)=\sum_{s=1}^{N_{Bus}}\left(V_{s(0)}-V_{s(NR+DG)}\right)^2\times 100 \quad (13)$$

where V_s is the s^{th} bus voltage.

3 Flow Direction Algorithm

Karami et al. Developed Flow Direction Algorithm (FDA) in 2021 using the D8 technique. The D8 algorithm determines the direction of water flow in a drainage basin after transforming the rainfall into runoff. Figure 2. Shows the basin outflow flow with the D8 technique. This method generates an original population in the drainage basin, which can also be considered the problem search space.

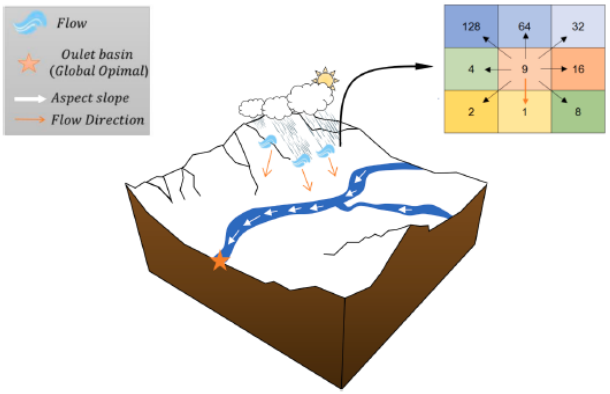

Fig. 2. Diagram of basin outflow flow with the D8 technique

Then, water flows are directed towards the lowest elevation area as much as possible, which can also be considered the best solution.

According to the FDA algorithm, the starting position of flows is calculated as follows:

$$X\_Flow(i)=lbrand\times(ub-lb) \tag{14}$$

X_Flow is the water flow position,

In addition to this, it is presumed that there are some β neighborhood flows around each flow; the neighboring flows are calculated as follows:

$$Neighbor(j)=X\_Flow(i)+\Delta\times randn \tag{15}$$

Where the neighbor represents the neighbor's position, The exploration will be limited to a small range if the value is minute; if the Δ value is large, the exploration will open up the possibility of exploring a broad range. In this algorithm, to enhance the probability of finding the closest to the optimal solutions (global search), search a wide range of search space that offers various solutions. It is also necessary to search a small region of the search space containing several optimal solutions to find the optimal global solution (local search) more accurately. If a global search process is enforced in the algorithm, the algorithm cannot discover the global optimum with the necessary precision; similarly, if a local process is enforced in the algorithm, the algorithm gets stuck with local optima. If a global search process is enforced in the algorithm, the algorithm cannot discover the global optimum with the necessary precision; similarly, if a local process is enforced in the algorithm, the algorithm gets stuck with local optima. Now, in this algorithm, the value of Δ was linearly reduced from the highest value to the smallest value to maintain the balance between global and local search; now, the direction of Δ is towards a random position for more variation. The mathematical modelling of Δ as follows:

$$\Delta=(rand\times X_{rand} - rand \times X\_Flow(i))\times\|X\_Best - X\_Flow\|\times W \tag{16}$$

X_{rand} is a random position, and W is a nonlinear weight with a random number between 0 and infinity. This first one describes that X_Flow (i) moves to a random position (X_{rand}). For the next one, by increasing iteration, Flow X(i) is closed to X_Best, and the Euclidian distance between X_Best and X_Flow (i) is reached to zero. The mathematical modelling of W is as follows:

$$W=\left(\left(1-\frac{iter}{Max\_iter}\right)^{(2\times randn)}\right)\times\left(rand\times\frac{iter}{Max\_iter}\right)\times rand \tag{17}$$

The changes of W while increasing the iterations are shown in Figure 3; this can avoid the stuck with local optima in the algorithm. All the water flows move with a velocity (V) to the neighbor with the minimum fitness function.

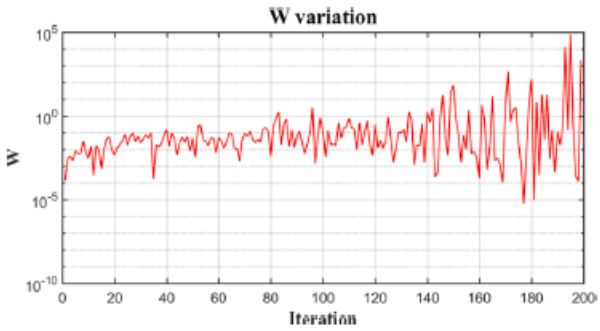

Fig. 3. The Changes of W.

The velocity of the water flow to neighbor flows depends on its slope. The mathematical modelling of V is as follows:

$$V=randn\times S_0 \tag{18}$$

The S_0 is the slope between the current and neighbor water flows; the randn generates numerous solutions and enhances global search capability. The following relation also determines the slope of i^{th} water flow to the neighbor j^{th}:

$$S(i,j,d)=\frac{Fitness\_Flow(i)-Neighbor\_Fitness(j)}{\|X\_Flow(i,d)-Neighbor(j,d)\|} \tag{19}$$

To find the new position of water flow, the mathematical modelling is as follows:

$$Flow\_Xnew(i)=Flow\_X(i)+V\times\frac{X\_Flow(i)-Neighbor(j)}{|X\_Flow(i)-Neighbor(j)|} \tag{20}$$

The fitness function of any neighbor may not be less than the new flow objective function, which is similar to the sink-filling process to determine the water flow direction. In this situation, the FDA algorithm chooses a new flow randomly; if its fitness function is less than the current flow's, it will follow the same path; otherwise, it will follow the prevailing slope direction. The position of a sink before and after filling is shown in Figure 4.

Modified Flow Direction Algorithm

In the case of population-based optimization, there may be a possibility of skipping the optimal solution when the global search process accelerates the convergence speed of the algorithm. The size of the local search process is crucial in determining how well an algorithm performs in terms of exploration and exploitation; meanwhile, a local search

process ensures adequate convergence accuracy. However, the balance between exploration and exploitation is necessary for an algorithm. Acceleration coefficients are introduced to maintain a proper balance between the exploration and exploitation of the FDA. This relationship determines the flow's new position:

$$Flow\_Xnew(i)=C_1.*Flow\_X(i)+C_2.*V\times\frac{X\_Flow(i)-Neighbor(j)}{|X\_Flow(i)-Neighbor(j)|} \quad (21)$$

Where C_1 and C_2 are the acceleration coefficients, which are equal to one, i.e., $C_1 + C_2 = 1$; these values were historically chosen as $C_1 = 0.1$ and $C_2 = 0.9$. The pseudo-code of MFDA is shown in Table 2, and the flow chart is shown in Figure 5.

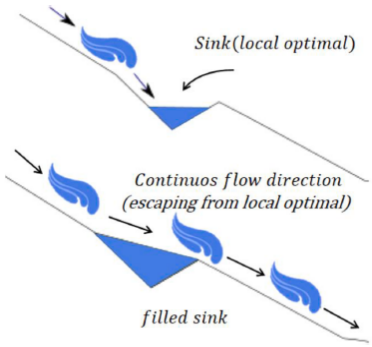

Fig. 4. Position of a sink before and after filling.

Under these conditions, the flow direction may be simulated using the following relation.

$$\begin{cases} Flow\_Xnew(i)=X\_Flow(i)+randn\times(X\_Flow(r)-X\_Flow(i)) & \text{if } Fitness\_Flow(r)<Fitness\_Flow(i) \\ Flow\_Xnew(i)=X\_Flow(i)+2randn\times(X\_Best-X\_Flow(i)) & \text{otherwise} \end{cases} \quad (22)$$

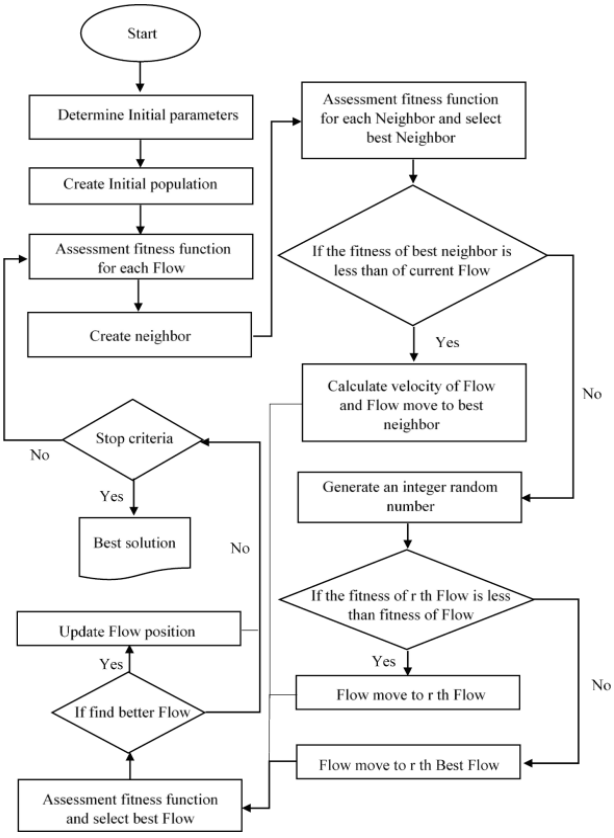

Fig. 5. Flowchart of MFDA

Table 2. Pseudo Code of MFDA

```
Initialize the search agents (X_Flow_i) i = 1, . . ., n
Compute the fitness function and create fitness matrix
Initialize the velocity of flows V_min and V_max
while it < itmax
    update the W using (Eq. 17)
    for all the flows
        for all the neighbours
            Initialize neighbourhood radius Δ_j; j = 1, . . ., β using (Eq. 16)
            Initialize neighbour flows X_ neighbour
            Compute the neighbour fitness function and create fitness matrix
            end (for all the neighbours)
            update the slope of neighbour using (Eq. 19)
            if neighbour fitness < flow fitness
                update the velocity of each flow using (Eq. 18)
                update the new flow using (Eq. 22)
            else
                update the new flow using (Eq. 21)
            end
            update the best flow and fitness function
    end (for all the flows)
end (while)
```

4. Simulation Results and Discussion

The proposed MFDA was applied to the sixteen benchmark functions and simultaneous reconfiguration and DG installation to prove effectiveness and robustness. This paper has taken the mean value and standard deviation of sixteen benchmark functions with 500 maximum iterations, 50 population sizes, and 30 independent runs for a fair comparison.

Table 3. Unimodal Functions

Function	Dim	Range	F_{min}
$F_1(x)=\sum_{i=1}^{dim} x_i^2$	30	-100, 100	0
$F_2(x)=\sum_{i=1}^{dim}\|x_i\|+\prod_{i=1}^{dim}\|x_i\|$	30	-10, 10	0
$F_3(x)=\sum_{i=1}^{dim}\left(\sum_{j-1}^{i} x_j^2\right)^2$	30	-100, 100	0
$F_4(x)=\max_i\{\|x_i\|, 1\le i\le dim\}$	30	-100, 100	0
$F_5(x)=\sum_{i=1}^{dim}\left[100\left(x_{i+1}-x_i^2\right)^2+(x_i-1)^2\right]$	30	-30, 30	0
$F_6(x)=\sum_{i=1}^{dim}(\|x_i+0.5\|)^2$	30	-100, 100	0
$F_7(x)=\sum_{i}^{dim} ix_i^4+rand(0,\ 1)$	30	-1.28, 1.28	0

4.1 Benchmark Functions

First, the proposed MFDA was applied to sixteen benchmark functions to prove effectiveness and robustness. The parameters of the MFDA algorithm are the same as [69]. Maximum iterations are 500, and the population size is 50 for the sixteen benchmark functions. The details of the unimodal and multimodal benchmark functions may be seen in Tables 3 and 4, respectively. The outcomes attained by the FDA [69], OFDA [74], and MFDA may be seen in Tables 5 and 6. Table 5 shows that the proposed MFDA performs better regarding the mean value and standard deviation. The results obtained by MFDA for the unimodal functions F1, F2, F3, F4, F5, and F7 give better results than FDA and OFDA; for the function, F6 is worse than the OFDA but better than FDA. The results obtained by MFDA for the multimodal functions F9, F10, F11, F15, and F16 give better results than FDA and OFDA, for the functions F8 and F12 are worse than the OFDA but better than the FDA, for the function F13 gives worse than FDA and OFDA. Table 6 shows that the proposed MFDA performs better regarding the success rate than the FDA and

OFDA. The convergence curves of some of the benchmark functions may be seen in Figure 6.

Table 4. Multimodal Functions

Function	Dim	Range	F_{min}
$F_8(x) = \sum_{i=1}^{dim} -x_i \sin\left(\sqrt{\lvert x_i \rvert}\right)$	30	-500, 500	-418.9829×5
$F_9(x) = \sum_{i=1}^{dim}\left[x_i^2 - 10\cos\left(2\prod x_i\right)+10\right]$	30	-5.12, 5.12	0
$F_{10}(x) = \sum_{i=1}^{dim} -20\exp\left(-0.2\sqrt{\frac{1}{dim}\sum_{i=dim}^{dim} x^2}\right) - \exp\left(\frac{1}{dim}\sum_{i=1}^{dim}\cos(2\prod x_i)\right) 20+e$	30	-32, 32	0
$F_{11}(x) = \frac{1}{4000}\sum_{i=1}^{n} x_i^2 - \prod_{i=1}^{n}\cos\left(\frac{x_i}{\sqrt{i}}\right)+1$	30	-600, 600	0
$F_{12}(x) = \frac{\pi}{n}\left\{10\sin(\pi y_1)+\sum_{i=1}^{n-1}(y_i-1)^2\left[1+10\sin^2(\pi y_{i+1})\right]+(y_n-1)^2\right\}+\sum_{i=1}^{n} u(x_i,10,100,4),\ y_i=1+\frac{x_i+1}{4}$	30	-50, 50	0
$F_{13}(x) = 0.1\left\{\sin^2(3\pi x_1)+\sum_{i=1}^{n}(x_i-1)^2\left[1+\sin^2(3\pi x_i+1)\right]+(x_n-1)^2\left[1+\sin^2(2\pi x_n)\right]\right\}+\sum_{i=1}^{n} u(x_i,5,100,4)$	30	-50, 50	0
$F_{14}(x) = -\sum_{i=1}^{n}\sin(x_i).\left(\sin\left(\frac{i.x_i^2}{\pi}\right)\right)^{2m}$, m = 10	30	0, π	-4.687
$F_{15}(x) = \left[e^{-\sum_{i=1}^{n}\left(x_i/\beta\right)^{2m}} - 2e^{-\sum_{i=1}^{n} x_i^2}\right].\prod_{i=1}^{n}\cos^2 x_i$, m=5	30	-20, 20	-1
$F_{16}(x) = 4x_1^2 - 2.1x_1^4+\frac{1}{3}x_1^6+x_1x_2-4x_2^2+4x_2^4$	30	-10, 10	-1
where $u(x_i,a,k,m)=\begin{cases} k(x_i-a)^m & x_i>a \\ 0 & -a<x_i<a \\ k(-x_i-a)^m & x_i<-a \end{cases}$			

Table 5. Outcomes of unimodal and multimodal functions

Function	FDA		OFDA		MFDA	
	Ave	Std	Ave	Std	Ave	Std
F1	9.00E-05	6.10E-05	1.90E-65	1.00E-64	**3.50E-160**	**1.90E-159**
F2	4.90E-04	2.70E-04	7.00E-19	3.60E-18	**9.40E-113**	**3.30E-112**
F3	4.90E+01	3.10E+01	5.30E-12	2.90E-11	**1.80E-153**	**7.00E-153**
F4	1.70E+01	2.90E+00	1.50E+01	3.40E+00	**1.10E-85**	**3.80E-85**
F5	6.50E+01	4.10E+01	2.30E+01	4.40E+00	**2.40E+01**	**7.00E-01**
F6	1.50E-04	2.20E-04	**0.00E+00**	**0.00E+00**	4.20E-06	6.10E-06
F7	9.50E-02	3.80E-02	3.70E-04	2.40E-04	**1.90E-04**	**1.40E-04**
F8	-3.30E+03	3.40E+02	**-3.60E+03**	**2.80E+02**	-3.40E+03	3.60E+02
F9	9.90E+00	3.40E+00	4.40E+00	6.90E+00	**0.00E+00**	**0.00E+00**
F10	1.20E-01	3.50E-01	4.20E-15	1.30E-15	**1.00E-15**	**6.50E-16**
F11	2.00E-01	1.20E-01	4.10E-02	4.40E-02	**0.00E+00**	**0.00E+00**
F12	2.10E-02	7.90E-02	**4.70E-32**	**1.70E-47**	2.30E-24	1.10E-23
F13	3.70E-04	2.00E-03	**3.90E-32**	**6.70E-32**	2.10E-02	3.90E-02
F14	**1.00E+00**	**0.00E+00**	**1.00E+00**	**0.00E+00**	1.90E+00	2.70E+00
F15	5.20E-04	3.90E-04	5.30E-04	3.90E-04	**3.10E-04**	**1.80E-19**
F16	-1.00E+00	6.80E-16	-1.00E+00	6.80E-16	**-1.00E+00**	**6.70E-16**

Table 6. Outcomes of success rate for unimodal and multimodal functions

Function	Threshold	FDA	OFDA	MFDA
		Success Rate	Success Rate	Success Rate
F1	1.00E-20	0	100	100
F2	1.00E-20	0	90	100
F3	1.00E-20	0	73.33	100
F4	1.00E-20	0	0	100
F5	1.00E-20	0	16.66	0
F6	1.00E-20	0	100	0
F7	1.00E-05	0	0	10
F8	1.00E-05	100	100	100
F9	1.00E-05	0	50	100
F10	1.00E-05	83.33	100	100
F11	1.00E-05	0	56.66	100
F12	1.00E-05	73.33	100	100
F13	1.00E-05	100	100	66.66
F14	1.00E-05	0	0	0
F15	1.00E-05	0	0	0
F16	1.00E-05	100	100	100
Average		28.54	61.67	**67.29**

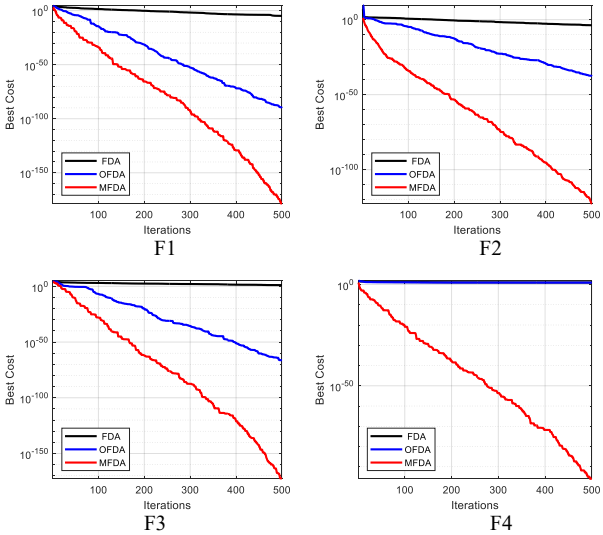

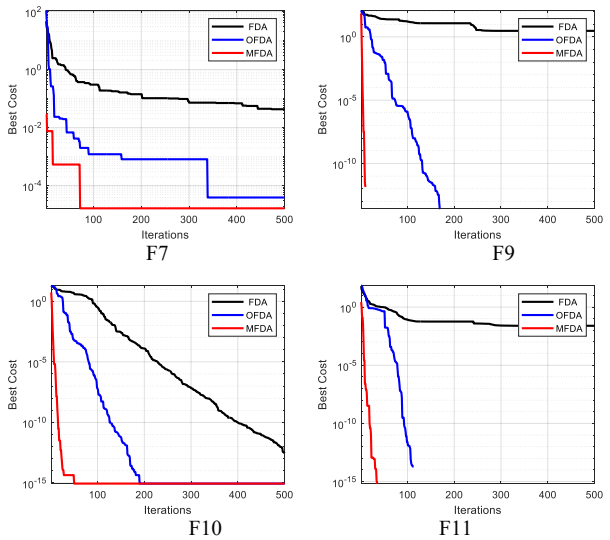

Fig. 6. Convergence curves of some of the benchmark functions

4.2 Network Reconfiguration with Distributed Generator Installation

Second, simultaneous reconfiguration and DG installation using 33-69 bus test systems to prove effectiveness and robustness. Distribution system total loss depends on integrated DG size and location, so adding more DGs may be technologically or financially unfeasible. DGs become active networks and increase network short-circuit levels if their overall rating increases. For a fair and accurate comparison, this study restricts the number of DGs to historical literature [35], [59], [60], but the suggested approach works for any number of DGs. To test the efficacy and superiority of the suggested method, we simulate all of the systems with three case studies under light (0.5), nominal (1.0), and heavy (1.6) load levels.

The parameters of the MFDA algorithm are the same as [59]. Maximum iterations are 500 for the 33 – 69 bus systems, and the population size is 75 for the 33 – 69 bus systems based on problem difficulty and size. The research cases are repeated 30 times, and the results are consistent every time, with negligible variations among various runs. MATLAB R2018a runs on a PC with 8 GB RAM and an 11th Gen Intel Core i5-11300H @ 3.10GHz processor.

4.3 Bus Systems

The test system data is taken at [46], [71], [72], [73]; this system contains five ties and 32 sectional switches. Figure 7 exhibits the single-line diagram of the test system. The active and reactive power demands and losses are (3.72 MW and 2.30 MVAr), (202.66 kW, and 135.14 kVAr), respectively, and the minimum voltage is 0.9131 (p.u.).

System network setup begins with the base case. Next, switches 33, 34, 35, 36, and 37 are opened, causing active (kW) and reactive (kVAr) power losses and minimum voltage (p.u.) for three loading conditions (47.07, 31.35, 0.9583 (18)), (202.66, 135.14, 0.9131 (18)) and (575.31, 384.26, 0.8529 (18)), respectively.

The second stage deals only with network reconfiguration to attain the best switch states; the attained best switch states are tabulated in Table 7. Table 7 shows that the MFDA finds optimal open switches for all three loads (7, 9, 14, 32, and 37). Table 7 shows that real (kW) and reactive (kVAr) power loss decreased to (33.27 and 24.38), (139.55 and 102.30), and (380.44 and 278.97) for the three loading scenarios. Active and reactive power loss index (%) are (29.32 and 22.22), (31.14 and 24.3), and (33.87 and 27.4) for each load condition. Table 7 shows that minimum system voltage has grown dramatically at different load levels. VPI (%) is 0.41, 1.84, and 5.61; these findings show that the MFDA effectively works for optimum network reconfiguration.

Table 7. For a 33-bus with different case studies and load levels.

Case	Description	Load Level		
		Light	**Nominal**	**Heavy**
Case 1	TP_{Loss} (kW)	47.07	202.66	575.31
	TQ_{Loss} (kVAr)	31.35	135.14	384.26
	V_{min} (p.u.)	0.9583 (18)	0.9131 (18)	0.8529 (18)
Case 2	Open Switches	7−9−14−32−37	7−9−14−32−37	7−9−14−32−37
	TP_{Loss} (kW)	33.27	139.55	380.44
	TQ_{Loss} (kVAr)	24.38	102.30	278.97
	APLRI (%)	29.32	31.14	33.87
	RPLRI (%)	22.22	24.3	27.4
	V_{min} (p.u.)	0.9698 (32)	0.9378 (32)	0.8967 (32)
	VPI (%)	0.41	1.84	5.61
Case 3	Size in kW (Bus)	371.5 (25) 371.5 (14) 371.5 (31)	743 (25) 743 (14) 743 (31)	1188.8 (14) 1188.8 (25) 1188.8 (31)
	TP_{Loss} (kW)	18.47	76.71	206.28
	TQ_{Loss} (kVAr)	12.51	51.95	139.73
	APLRI (%)	60.77	62.15	64.15
	RPLRI (%)	60.11	61.56	63.64
	V_{min} (p.u.)	0.9811 (33)	0.9612 (33)	0.9359 (33)
	VPI (%)	0.85	3.77	11.13
Case 4	Open Switches	7−28−34−35−36	7−28−34−35−36	7−11−14−28−36
	Size in kW (Bus)	371.50 (32) 371.50 (29) 371.50 (8)	743.00 (30) 743.00 (15) 743.00 (25)	1188.8 (31) 1188.8 (9) 1158.8 (25)
	TP_{Loss} (kW)	14.12	58.36	154.38
	TQ_{Loss} (kVAr)	11.15	43.31	114.71
	APLRI (%)	70	71.2	73.17
	RPLRI (%)	64.43	67.96	70.15
	V_{min} (p.u.)	0.9815 (17)	0.9724 (33)	0.9574 (33)
	VPI (%)	1.08	5.88	18.31

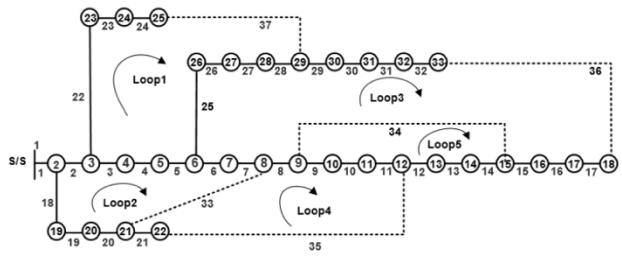

Fig. 7. IEEE-33 bus base configuration

In the third stage, the system installs the only optimal DG to attain the optimal size and location of DG; the obtained optimal DG sizes and locations are tabulated in Table 7. From Table 7, it is observed that the MFDA finds the best optimal locations for all three loads (25, 14, 31), (25, 14, 31), and (14, 25, 31) with real power injection capacities in kW (371.5, 371.5, 371.5), (743, 743, 743), and (1188.8, 1188.8, 1188.8), respectively. Table 7 shows that active (kW) and reactive (kVAr) power loss decreases to (18.47, 12.51), (76.71, 51.95), and (206.28, 139.73) for the three loading conditions. Active and reactive power loss indexes (%) are (60.77, 60.11), (62.15, 61.56), and (64.15, 63.64) for each loading state. Table 7 shows that minimum system voltage has grown dramatically at different load levels. VPI (%) is 0.85, 3.77, and 11.13; these findings show that the MFDA effectively works for appropriate DG installation.

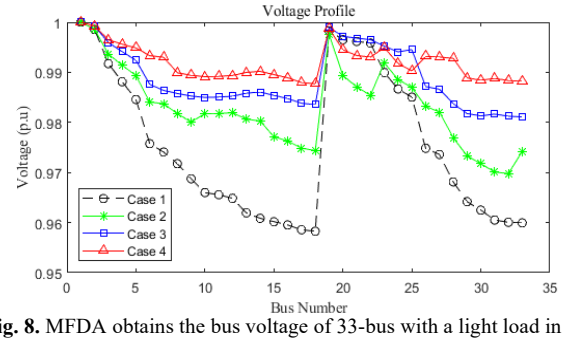

Fig. 8. MFDA obtains the bus voltage of 33-bus with a light load in all cases.

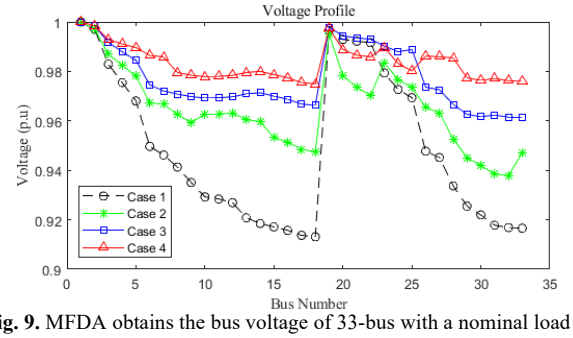

Fig. 9. MFDA obtains the bus voltage of 33-bus with a nominal load in all cases.

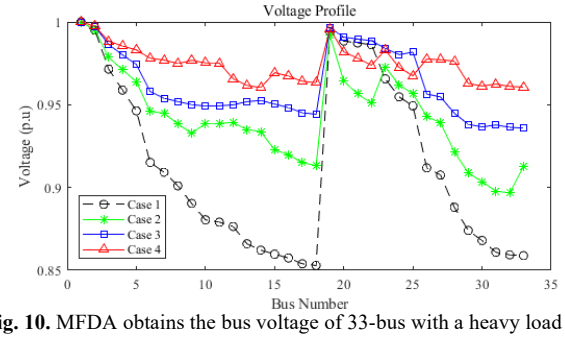

Fig. 10. MFDA obtains the bus voltage of 33-bus with a heavy load in all cases.

In the fourth stage, reconfiguration and DG installation are performed simultaneously for the system to attain an optimal state of switches, size, and location of DG; attained best switch states, size, and location of DG are tabulated in Table 7, and this table shows that the MFDA attained the best open switches for all three load (7, 28, 34, 35 and 36), (7, 28, 34, 35 and 36), and (7, 11, 14, 28, and 36) and best optimal locations for all three loads (32, 29, and 8), (30, 15, and 25), and (31, 9, and 25) with real power injection capacities in kW (371.5, 371.5, and 371.5), (743, 743, and 743), and (1188.8, 1188.8, and 1158.8), respectively. Table 7 shows that power loss decreases for real (kW) and reactive (kVAr) loading conditions by (14.12 and 11.15), (58.36 and 43.31), and (154.38 and 114.71) for the three loading conditions. Active and reactive power loss indexes (%) are (70, 64.43), (71.2, 67.96), and (73.17, 70.15) for each loading state. Table 6 shows that minimum system voltage has grown dramatically at different load levels. VPI (%) is 1.08, 5.88, and 18.31; these findings show that the MFDA effectively works for simultaneous reconfiguration and DG installation. The convergence curve of the light, nominal, and heavy loads is shown in Figures 11(a), 11(b), and 11(c) for the cases.

To show the relevance of the suggested approach, Tables 8, 9, and 10 compare the MFDA performance to ISCA [2] and FWA [3] results in all three loading situations. The tables show that the MFDA is best.

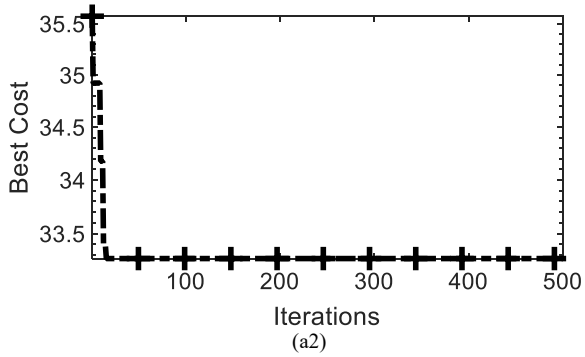

(a2)

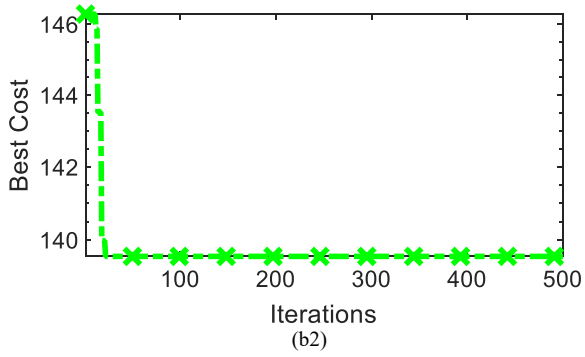

(b2)

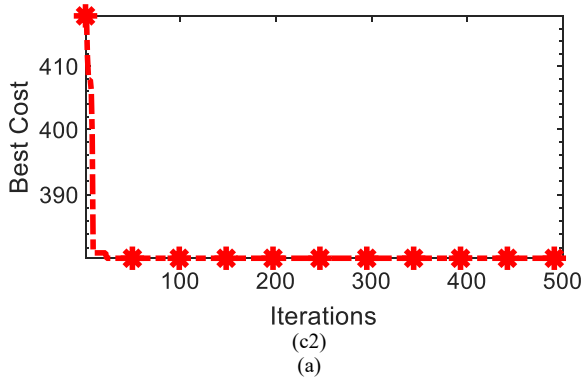

(c2)

(a)

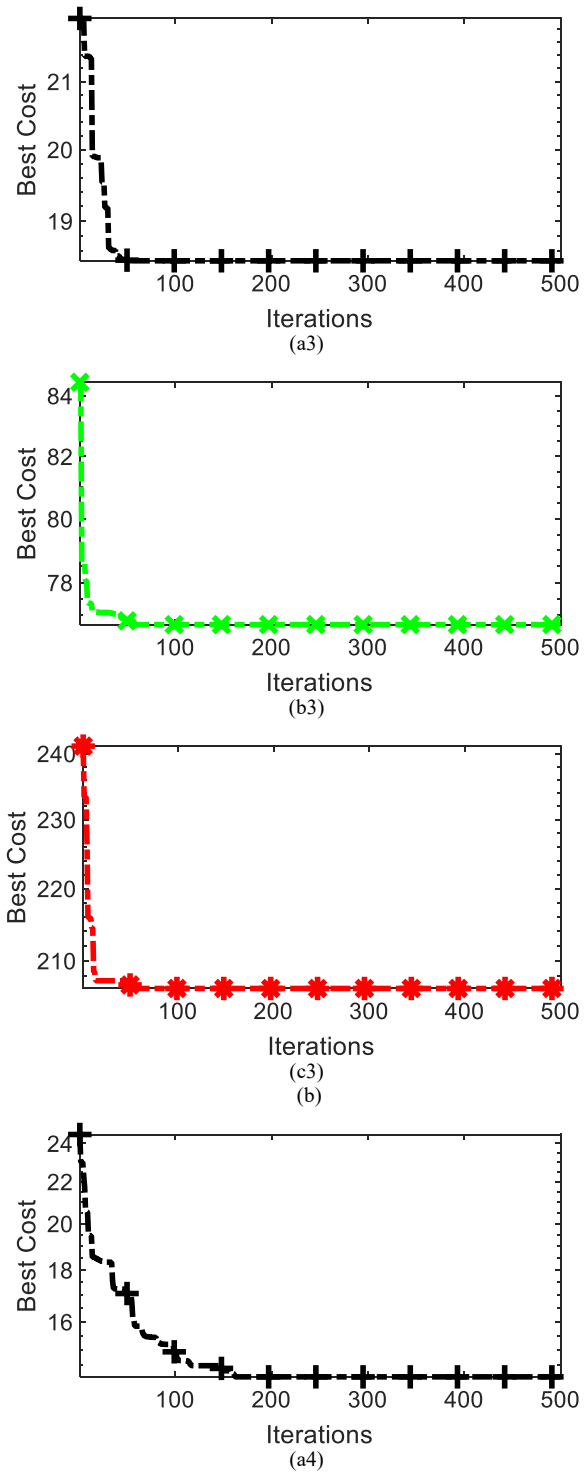

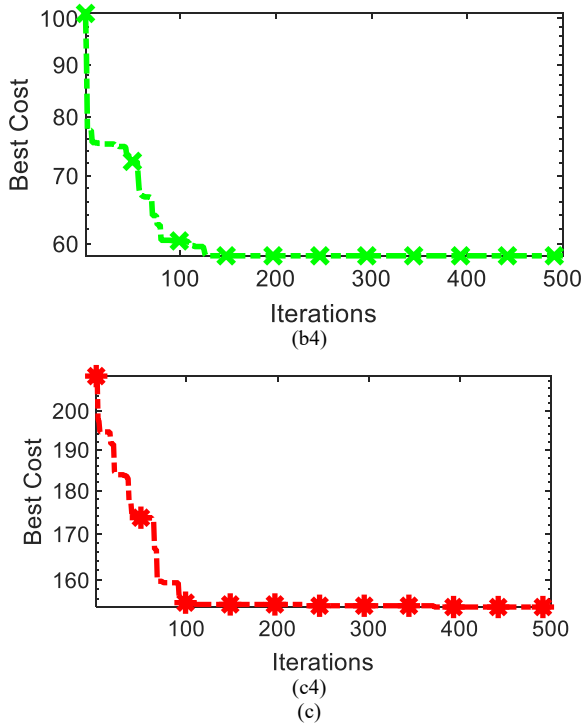

Fig. 11. (a) Convergence curve of the light, nominal, and heavy load conditions for case 2, (b) convergence curve of the light, nominal, and heavy load conditions for case 3 and (c) convergence curve of the light, nominal, and heavy load conditions for case 4

In case 3, APLRI obtained by the MFDA is 62.15%, which is better than ISCA [2], HSA [46], FWA [3], GA [46], RGA [46], and FF [70]. The value of RPLRI obtained from the MFDA is 61.56%, which is better than ISCA [2], HSA [46], and FWA [3]; thus, the MFDA achieves better results than other algorithms on all three measures.

The performance of the MFDA is compared across all cases of ISCA [2], HSA [46], FWA [3], GA [46], RGA [46], and FF [70] at the nominal loading conditions, and the outcomes are provided in Table 11. In case 2, as shown in the table, APLRI produced by the MFDA is 31.14%, identical to those gained by ISCA [2]. The MFDA produces superior outcomes compared to HSA [46], FWA [3], GA [46], and RGA [46]. RPLRI produced by the MFDA is 24.3% identical to those gained by ISCA [2] and FWA [3] and worse than HSA [46]. The minimum voltage obtained by the MFDA is 0.9378, identical to those gained by ISCA [2] and FWA [3]. The MFDA produces superior outcomes compared to HSA [46], GA [46], and RGA [46]. Thus, the MFDA achieves better results than other algorithms on all three measures.

In case 4, APLRI obtained by the MFDA is 71.2%, which is better than ISCA [2], HSA [46], FWA [3], GA [46], RGA [46], and FF [70]. The value of RPLRI obtained from the MFDA is 67.96%, which is better than ISCA [2], HSA [46], and FWA [3]; thus, the MFDA achieves better results than other algorithms on all three measures.

Table 8. For a 33-bus with a light load, MFDA is compared against other algorithms.

Case	Description	FWA [3]	ISCA [2]	MFDA
Case 1	TP_{Loss} (kW)	47.06	47.067	47.07
	TQ_{Loss} (kVAr)	-	31.35	31.35
	V_{min} (p.u.)	0.9583 (18)	0.9583 (18)	0.9583 (18)
Case 2	Open Switches	7−14−9−32−28	37−32−9−14−7	7−9−14−32−37
	TP_{Loss} (kW)	33.39	33.26	33.27
	TQ_{Loss} (kVAr)	-	24.38	24.38
	APLRI (%)	29.04	29.33	29.32

	RPLRI (%)	-	22.23	22.22
	V_{min} (p.u.)	0.9714 (32)	0.9698 (33)	0.9698 (32)
	VPI (%)	-	0.41	0.41
Case 3	Size in kW (Bus)	294.80 (14) 94.700 (18) 507.20 (32)	371.50 (14) 371.50 (24) 371.50 (31)	371.5 (25) 371.5 (14) 371.5 (31)
	TP_{Loss} (kW)	21.37	18.57	18.47
	TQ_{Loss} (kVAr)	-	12.58	12.51
	APLRI (%)	54.58	60.55	60.77
	RPLRI (%)	-	59.87	60.11
	V_{min} (p.u.)	0.9844 (30)	0.9811 (33)	0.9811 (33)
	VPI (%)	-	0.85	0.85
Case 4	Open Switches	7−14−10−32−28	7−10−14−31−28	7−28−34−35−36
	Size in kW (Bus)	258.60 (32) 321.80 (29) 280.30 (18)	357.98 (30) 88.670 (13) 340.11 (16)	371.50 (32) 371.50 (29) 371.50 (8)
	TP_{Loss} (kW)	16.22	16.24	14.12
	TQ_{Loss} (kVAr)	-	12.14	11.15
	APLRI (%)	65.53	65.49	70
	RPLRI (%)	-	61.28	64.43
	V_{min} (p.u.)	0.9862 (14)	0.9816 (32)	0.9815 (17)
	VPI (%)	-	1.08	1.08

Table 9. For a 33-bus with a nominal load, MFDA is compared against other algorithms.

Case	Description	FWA [3]	ISCA [2]	MFDA
	TP_{Loss} (kW)	202.67	202.66	202.66
Case 1	TQ_{Loss} (kVAr)	-	135.14	135.14
	V_{min} (p.u.)	0.9131 (18)	0.9131 (18)	0.9131 (18)
	Open Switches	7−14−9−32−28	7−14−9−32−28	7−9−14−32−37
	TP_{Loss} (kW)	139.98	139.55	139.55
	TQ_{Loss} (kVAr)	-	102.30	102.30
Case 2	APLRI (%)	30.93	31.14	31.14
	RPLRI (%)	-	24.30	24.3
	V_{min} (p.u.)	0.9413 (32)	0.9378 (32)	0.9378 (32)
	VPI (%)	-	1.27	1.84
	Size in kW (Bus)	589.70 (14) 189.50 (18) 1014.6 (32)	743.00 (14) 743.00 (24) 743.00 (31)	743 (25) 743 (14) 743 (31)
	TP_{Loss} (kW)	88.68	77.13	76.71
Case 3	TQ_{Loss} (kVAr)	-	52.29	51.95
	APLRI (%)	56.24	61.94	62.15
	RPLRI (%)	-	61.31	61.56
	V_{min} (p.u.)	0.9680 (30)	0.9612 (33)	0.9612 (33)
	VPI (%)	-	3.8	3.77
Case 4	Open Switches	7−14−11−32−28	7−9−14−28−31	7−28−34−35−36
	Size in kW (Bus)	536.70 (32) 615.80 (29) 531.50 (18)	648.46 (30) 510.27 (13) 532.46 (16)	743.00 (30) 743.00 (15) 743.00 (25)
	TP_{Loss} (kW)	67.11	66.81	58.36
	TQ_{Loss} (kVAr)	-	49.53	43.31
	APLRI (%)	66.89	67.03	71.2
	RPLRI (%)	-	63.35	67.96
	V_{min} (p.u.)	0.9713 (14)	0.9611 (31)	0.9724 (33)
	VPI (%)	-	5.14	5.88

Table 10. For a 33-bus with a heavy load, MFDA is compared against other algorithms.

Case	Description	FWA [3]	ISCA [2]	MFDA
	TP_{Loss} (kW)	575.31	575.31	575.31
Case 1	TQ_{Loss} (kVAr)	-	384.25	384.26
	V_{min} (p.u.)	0.8529 (18)	0.8529 (18)	0.8529 (18)
	Open Switches	7−14−9−32−28	7−9−14−37−32	7−9−14−32−37
Case 2	TP_{Loss} (kW)	381.24	380.44	380.44
	TQ_{Loss} (kVAr)	-	278.96	278.97
	APLRI (%)	33.73	33.87	33.87

	RPLRI (%)	-	27.39	27.4
	V_{min} (p.u.)	0.9027 (32)	0.8967 (32)	0.8967 (32)
	VPI (%)	-	5.61	5.61
Case 3	Size in kW (Bus)	944.10 (14) 301.30 (18) 1678.4 (32)	1188 (14) 1188 (24) 1188 (31)	1188.8 (14) 1188.8 (25) 1188.8 (31)
	TP_{Loss} (kW)	238.07	207.49	206.28
	TQ_{Loss} (kVAr)	-	140.66	139.73
	APLRI (%)	58.57	63.93	64.15
	RPLRI (%)	-	63.39	63.64
	V_{min} (p.u.)	0.9484 (29)	0.9359 (33)	0.9359 (33)
	VPI (%)	-	11.08	11.13
Case 4	Open Switches	7−14−11−32−28	7−9−14−28−31	7−11−14−28−36
	Size in kW (Bus)	959.00 (32) 1190.1 (29) 1020.6 (18)	1126.80 (30) 700.600 (13) 1153.80 (16)	1188.8 (31) 1188.8 (9) 1158.8 (25)
	TP_{Loss} (kW)	172.97	167.96	154.38
	TQ_{Loss} (kVAr)	-	123.9	114.71
	APLRI (%)	69.93	70.81	73.17
	RPLRI (%)	-	67.76	70.15
	V_{min} (p.u.)	0.9554 (14)	0.9504 (32)	0.9574 (33)
	VPI (%)	-	17.09	18.31

Table 11. For a 33-bus with a nominal load, MFDA is compared against other algorithms.

Method	Description	Case 2	Case 3	Case 4
MFDA	Open Switches	7−9−14−32−37	33−34−35−36−37	7−10−12−28−32
	Size in kW (Bus)	-	2229	2229
	APLRI (%)	31.14	62.15	71.2
	RPLRI (%)	24.30	61.56	67.96
	V_{min} (p.u.)	0.9378 (32)	0.9612 (33)	0.9724 (18)
ISCA [2]	Open Switches	7−14−9−32−37	33−34−35−36−37	7−9−14−28−31
	Size in kW (Bus)	-	2229	1691.2
	APLRI (%)	31.14	61.94	67.03
	RPLRI (%)	24.30	61.31	63.35
	V_{min} (p.u.)	0.9378	0.9612	0.9611
HSA [46]	Open Switches	7−14−9−32−37	33−34−35−36−37	7−4−10−32−28
	Size in kW (Bus)	-	1725.6	1668.4
	APLRI (%)	31.88	52.26	63.95
	RPLRI (%)	24.3	48.38	55.73
	V_{min} (p.u.)	0.9342	0.9670	0.9700
FWA [3]	Open Switches	7−14−9−32−28	33−34−35−36−37	7−14−11−32−28
	Size in kW (Bus)	-	1793.7	1684.1
	APLRI (%)	30.93	56.24	66.89
	RPLRI (%)	22.39	55.13	62.78
	V_{min} (p.u.)	0.9413	0.9680	0.9713
GA [46]	Open Switches	33−34−9−36−28	33−34−35−36−37	7−34−10−32−28
	Size in kW (Bus)	-	1604.4	1963.3
	APLRI (%)	30.15	50.60	62.92
	RPLRI (%)	-	-	-
	V_{min} (p.u.)	0.9310	0.9605	0.9766
RGA [46]	Open Switches	7−14−9−32−37	33−34−35−36−37	7−12−9−32−27
	Size in kW (Bus)	-	1777	1774
	APLRI (%)	31.20	51.84	63.33
	RPLRI (%)	24.3	-	-
	V_{min} (p.u.)	0.9315	0.9687	0.9691
FF [70]	Open Switches	-	33−34−35−36−37	8−9−28−32−33
	Size in kW (Bus)	-	-	1773.8
	APLRI (%)	-	-	63.51
	RPLRI (%)	-	-	59.35
	V_{min} (p.u.)	-	-	0.9735

In the same way, the performance of MFDA is compared to that of ISCA [2], HSA [46], and FWA [3] at the heavy loading condition. The outputs are summarized in Table 11. In cases 2, 3, and 4, the results indicate that the APLRI% and RPLRI% achieved by the MFDA are significantly superior to

those obtained by the ISCA [2], HSA [46], and FWA [3] in cases 2, 3, and 4. Thus, the MFDA achieves better results than other algorithms on all three measures. Figure 8, 9, and 10 displays the voltage profiles of light, nominal, and heavy for all the cases like the base case, light, nominal, and heavy load conditions attained by the proposed MFDA.

Table 12. For a 33-bus with a heavy load, MFDA is compared against other algorithms.

Method	Description	Case 2	Case 3	Case 4
MFDA	Open Switches	7−9−14−32−37	33−34−35−36−37	6−11−14−16−28
	Size in kW (Bus)	-	3566.4	3567
	APLRI (%)	33.87	64.15	73.17
	RPLRI (%)	27.40	63.64	70.15
	V_{min} (p.u.)	0.8967(32)	0.9359 (33)	0.9574 (14)
ISCA [2]	Open Switches	7−14−9−32−37	33−34−35−36−37	7−9−14−28−31
	Size in kW (Bus)	-	3564	2981.2
	APLRI (%)	33.87	63.93	70.81
	RPLRI (%)	27.39	63.39	67.76
	V_{min} (p.u.)	0.8967	0.9359	0.9504
HSA [46]	Open Switches	7−14−9−32−37	33−34−35−36−37	7−14−10−28−32
	Size in kW (Bus)	-	2716.2	2752.9
	APLRI (%)	33.86	54.63	66.23
	RPLRI (%)	27.39	51.32	61.50
	V_{min} (p.u.)	0.8967	0.9437	0.9516
FF [70]	Open Switches	7−14−9−32−28	33−34−35−36−37	7−4−10−32−28
	Size in kW (Bus)	-	2923.8	3169.7
	APLRI (%)	33.73	58.57	69.93
	RPLRI (%)	25.63	57.51	65.67
	V_{min} (p.u.)	0.9027	0.9484	0.9554

4.4 Bus Systems

The test system data is taken at [46], [71], [72], [73]; this system contains five ties and 68 sectional switches. Figure 12 exhibits the single-line diagram of the test system. The active and reactive power demands and losses are (3.8 MW and 2.69 MVAr), (225 kW and 102.16 kVAr), respectively, and the minimum voltage is 0.9092 (p.u.).

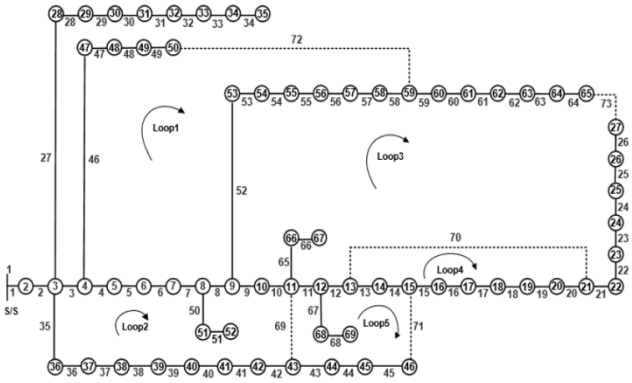

Fig. 12. IEEE-69 bus base configuration

System network setup begins with the base case. Next, switches 69, 70, 71, 72, and 73 are opened, causing active (kW) and reactive (kVAr) power losses and minimum voltage (p.u.) for three loading conditions (51.61, 23.55, 0.9567 (65)), (225, 102.16, 0.9092 (65)) and (652.53, 294.26, 0.8445 (65)), respectively.

The second stage deals only with network reconfiguration to attain the best switch states, tabulated in Table 13. From Table 13, it is observed that the MFDA finds optimal open switches for all three loads (14, 55, 61, 69, and 70), (14, 57, 61, 69, and 70), and (14, 56, 61, 69, and 70). Table 13 shows that real (kW) and reactive (kVAr) power loss decreased to (23.61 and 22.09), (98.61 and 92.05), and (267.11 and 248.64) for the three loading scenarios. Active and reactive power loss index (%) are (54.25 and 6.21), (56.18 and 9.9), and (59.06 and 15.5) for each load condition. Table 13 shows that minimum system voltage has grown dramatically at different load levels. VPI (%) is 0.67, 3.37, and 9.45; these findings show that the MFDA effectively works for optimum network reconfiguration.

In the third stage, the system installs the only optimal DG to attain the optimal size and location of DG; the obtained optimal DG sizes and locations are tabulated in Table 13, and this table displays that the MFDA finds the best optimal locations for all three loads (17, 61, and 62), (62, 61, and 17), and (17, 61, and 62) with real power injection capacities in kW (279.8, 380.2, and 380.2), (760.4, 760.4, and 569.7) and (932.7, 1216.7, and 1216.7) respectively. Table 13 shows that active (kW) and reactive (kVAr) power loss decreases to (18.05, 9.06), (74.11, 37.10), and (196.26, 97.84) for the three loading conditions. Active and reactive power loss indexes (%) are (65.03, 61.52), (67.06, 63.69), and (69.92, 66.75) for each loading state. Table 13 shows that minimum system voltage has grown dramatically at different load levels. VPI (%) is 1.08, 4.8, and 14.26; these findings show that the MFDA effectively works for appropriate DG installation.

In the fourth stage, reconfiguration and DG installation are performed simultaneously for the system to attain an optimal state of switches, size, and location of DG; attained best switch states, size, and location of DG are summarized in Table 13, and this table displays the MFDA attained the best open switches for all three load (12, 55, 63, 69, and 70), (12, 55, 62, 69, and 70), and (12, 55, 62, 69, and 70) and best optimal locations for all three loads (61, 62, and 65), (61, 62, and 65), and (61, 65, and 62) with real power injection capacities in kW (380, 339.6, and 249.2), (760, 688.3, and 500.8), and (1217, 806.2, and 1119), respectively. Table 13 shows that power loss decreases for real (kW) and reactive (kVAr) loading conditions by (9.6 and 8.99), (39.1 and 36.59), and (102.31 and 95.67) for the three loading conditions. Active and reactive power loss indexes (%) are (81.39, 61.82), (82.62, 64.19), and (84.35, 67.49) for each

loading state. Table 13 shows that minimum system voltage has grown dramatically at different load levels. VPI (%) is 1.37, 6.11, and 18.32; these findings show that the MFDA effectively works for simultaneous reconfiguration and DG installation.

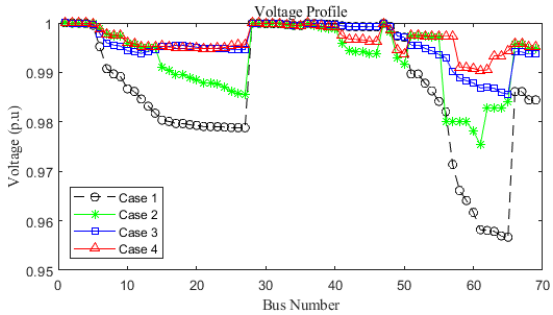

Fig. 13. MFDA obtains the bus voltage of 69-bus with a light load in all cases.

Table 13. For a 69-bus with different case studies and load levels.

Case	Description	Load Level		
		Light	**Nominal**	**Heavy**
Case 1	TP_{Loss} (kW)	51.61	225	652.53
	TQ_{Loss} (kVAr)	23.55	102.16	294.26
	V_{min} (p.u.)	0.9567 (65)	0.9092 (65)	0. 8445 (65)
Case 2	Open Switches	14−55−61− 69− 70	14− 57− 61− 69− 70	14− 56− 61− 69− 70
	TP_{Loss} (kW)	23.61	98.61	267.11
	TQ_{Loss} (kVAr)	22.09	92.05	248.64
	APLRI (%)	54.25	56.18	59.06
	RPLRI (%)	6.21	9.9	15.5
	V_{min} (p.u.)	0.9754 (61)	0.9495 (61)	0. 9165 (61)
	VPI (%)	0.67	3.37	9.45
Case 3	Size in kW (Bus)	279.8 (17) 380.2 (61) 380.2 (62)	760.4 (62) 760.4 (61) 569.7 (17)	932.7 (17) 1216.7 (61) 1216.7 (62)
	TP_{Loss} (kW)	18.05	74.11	196.26
	TQ_{Loss} (kVAr)	9.06	37.10	97.84
	APLRI (%)	65.03	67.06	69.92
	RPLRI (%)	61.52	63.69	66.75
	V_{min} (p.u.)	0. 9856 (65)	0.9705 (65)	0.9513 (65)
	VPI (%)	1.08	4.8	14.26
Case 4	Open Switches	12−55−63−69−70	12−55−62−69−70	12−55−62−69−70
	Size in kW (Bus)	380 (61) 339.6 (62) 249.2 (65)	760 (61) 688.3 (62) 500.8 (65)	1217 (61) 806.2 (65) 1119 (62)
	TP_{Loss} (kW)	9.6	39.1	102.31
	TQ_{Loss} (kVAr)	8.99	36.59	95.67
	APLRI (%)	81.39	82.62	84.32
	RPLRI (%)	61.82	64.19	67.49
	V_{min} (p.u.)	0. 9903 (61)	0. 9806 (61)	0. 9687 (61)
	VPI (%)	1.37	6.11	18.32

Table 14. For a 69-bus with a light load, MFDA is compared against other algorithms.

Case	Description	FWA [3]	ISCA [2]	MFDA
Case 1	TP_{Loss} (kW)	51.60	51.6	51.61
	TQ_{Loss} (kVAr)	-	23.55	23.55
	V_{min} (p.u.)	0.9567 (65)	0.9567 (65)	0.9567 (65)
Case 2	Open Switches	69−70−14−56−61	14−69−61−70−55	14−55−61−69−70
	TP_{Loss} (kW)	23.61	23.61	23.61
	TQ_{Loss} (kVAr)	-	22.08	22.09
	APLRI (%)	54.24	54.24	54.25
	RPLRI (%)	-	6.24	6.21
	V_{min} (p.u.)	0.9754 (61)	0.9754 (61)	0.9754 (61)
	VPI (%)	-	0.67	0.67
Case 3	Size in kW (Bus)	206.7 (65) 590.3 (61) 107.6 (27)	380.2 (12) 380.2 (62) 380.2 (61)	279.8 (17) 380.2 (61) 380.2 (62)
	TP_{Loss} (kW)	19.05	18.14	18.05
	TQ_{Loss} (kVAr)	-	9.02	9.06

	APLRI (%)	60.08	64.84	65.03
	RPLRI (%)	-	61.7	61.52
	V_{min} (p.u.)	0.9871 (62)	0.9862 (65)	0. 9856 (65)
	VPI (%)	-	0.97	1.08
Case 4	Open Switches	69−70−13−56−63	62−69−17−57−12	12−55−63−69−70
	Size in kW (Bus)	571.5 (61) 155.5 (62) 212.9 (64)	322.78 (61) 354.06 (62) 295.97 (65)	380 (61) 339.6 (62) 249.2 (65)
	TP_{Loss} (kW)	9.58	10.02	9.6
	TQ_{Loss} (kVAr)	-	9.32	8.99
	APLRI (%)	81.43	80.58	81.39
	RPLRI (%)	-	60.42	61.82
	V_{min} (p.u.)	0.9905 (61)	0.9894 (61)	0. 9903 (61)
	VPI (%)	-	1.45	1.37

Table 15. For a 69-bus with a nominal load, MFDA is compared against other algorithms.

Case	Description	FWA [3]	ISCA [2]	MFDA
Case 1	TP_{Loss} (kW)	224.96	225	225
	TQ_{Loss} (kVAr)	-	102.165	102.16
	V_{min} (p.u.)	0.9092 (65)	0.9092 (65)	0.9092 (65)
Case 2	Open Switches	69−70−14−56−61	15−55−61−69−70	14−57−61−69−70
	TP_{Loss} (kW)	98.59	98.60	98.61
	TQ_{Loss} (kVAr)	-	92.04	92.05
	APLRI (%)	56.17	56.18	56.18
	RPLRI (%)	-	9.91	9.9
	V_{min} (p.u.)	0.9495 (61)	0.9495 (61)	0.9495 (61)
	VPI (%)	-	3.01	3.37
Case 3	Size in kW (Bus)	408.5 (65) 1198.6 (61) 225.8 (27)	760.4 (12) 760.4 (62) 760.4 (61)	760.4 (62) 760.4 (61) 569.7 (17)
	TP_{Loss} (kW)	77.85	74.4	74.11
	TQ_{Loss} (kVAr)	-	36.93	37.10
	APLRI (%)	65.39	66.93	67.06
	RPLRI (%)	-	63.85	63.69
	V_{min} (p.u.)	0.9740 (62)	0.9717 (65)	0.9705 (65)
	VPI (%)	-	4.27	4.8
Case 4	Open Switches	69−70−13−55−63	12−19−69−63−57	12−55−62−69−70
	Size in kW (Bus)	1127.2 (61) 275.00 (62) 415.90 (65)	1000.9 (61) 410.60 (62) 461.60 (65)	760 (61) 688.3 (62) 500.8 (65)
	TP_{Loss} (kW)	39.25	39.73	39.1
	TQ_{Loss} (kVAr)	-	37.48	36.59
	APLRI (%)	82.55	82.34	82.62
	RPLRI (%)	-	63.31	64.19
	V_{min} (p.u.)	0.9796 (61)	0.9798 (61)	0. 9806 (61)
	VPI (%)	-	5.9	6.11

Table 16. For a 69-bus with a heavy load, MFDA is compared against other algorithms.

Case	Description	FWA [3]	ISCA [2]	MFDA
Case 1	TP_{Loss} (kW)	652.42	652.52	652.53
	TQ_{Loss} (kVAr)	-	294.26	294.26
	V_{min} (p.u.)	0.8445 (65)	0.8445 (65)	0. 8445 (65)
Case 2	Open Switches	69−70−14−56−61	14−55−61−69−70	14−56−61−69−70
	TP_{Loss} (kW)	267.08	267.11	267.11
	TQ_{Loss} (kVAr)	-	248.63	248.64
	APLRI (%)	59.06	59.06	59.06
	RPLRI (%)	-	15.51	15.5
	V_{min} (p.u.)	0.9165 (61)	0.9165 (61)	0. 9165 (61)
	VPI (%)	-	9.15	9.45
Case 3	Size in kW (Bus)	653.700 (65) 1917.70 (61) 361.300 (27)	1216.8 (12) 1216.8 (62) 1216.8 (61)	932.7 (17) 1216.7 (61) 1216.7 (62)

	TP_{Loss} (kW)	206.49	196.74	196.26
	TQ_{Loss} (kVAr)	-	97.32	97.84
	APLRI (%)	68.35	69.85	69.92
	RPLRI (%)	-	66.93	66.75
	V_{min} (p.u.)	0.9568 (62)	0.9530 (65)	0.9513 (65)
	VPI (%)	-	12.66	14.26
Case 4	Open Switches	69−70−13−57−63	69−70−14−55−62	12−55−62−69−70
	Size in kW (Bus)	1817.6 (61) 509.50 (62) 634.20 (65)	1600 (61) 510.9 (62) 634 (65)	1217 (61) 806.2 (65) 1119 (62)
	TP_{Loss} (kW)	102.97	104.5	102.31
	TQ_{Loss} (kVAr)	-	100.68	95.67
	APLRI (%)	84.21	83.99	84.32
	RPLRI (%)	-	65.79	67.49
	V_{min} (p.u.)	0.9685 (61)	0.9638 (61)	0. 9687 (61)
	VPI (%)	-	16.57	18.32

The performance of the MFDA is compared across all cases of ISCA [2], HSA [46], FWA [3], GA [46], and RGA [46] at the nominal loading conditions, and the outcomes are provided in Table 17. In case 2, as shown in the table, APLRI produced by the MFDA is 56.18%, identical to those gained by ISCA [2]. The MFDA produces superior outcomes compared to HSA [46], FWA [3], GA [46], and RGA [46]. RPLRI produced by the MFDA algorithm is 9.9% identical to those gained by ISCA [2] and FWA [3] and worse than HSA [46]. The minimum voltage obtained by the MFDA is 0.9495, identical to those gained by ISCA [2] and FWA [3]. The MFDA produces superior outcomes compared to HSA [46], GA [46], and RGA [46]. Thus, the MFDA achieves better results than other algorithms on all three measures.

In case 3, APLRI obtained by the MFDA is 67.06%, which is better than ISCA [2], HSA [46], FWA [3], GA [46], and RGA [46]. The value of RPLRI obtained from the MFDA is 63.69%, which is better than ISCA [2], HSA [46], and FWA [3]; thus, the MFDA achieves better results than other algorithms on all three measures.

In case 4−APLRI obtained by the MFDA is 82.32%, which is better than ISCA [2], HSA [46], FWA [3], GA [46], and RGA [46]. The value of RPLRI obtained from the MFDA is 64.19%, which is better than ISCA [2], HSA [46], and FWA [3]; thus, the MFDA achieves better results than other algorithms on all three measures.

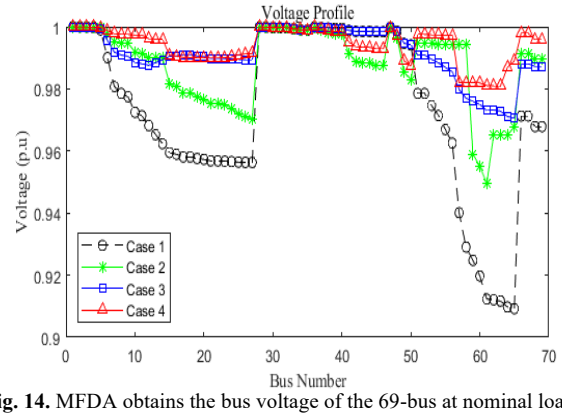

Fig. 14. MFDA obtains the bus voltage of the 69-bus at nominal load in all cases.

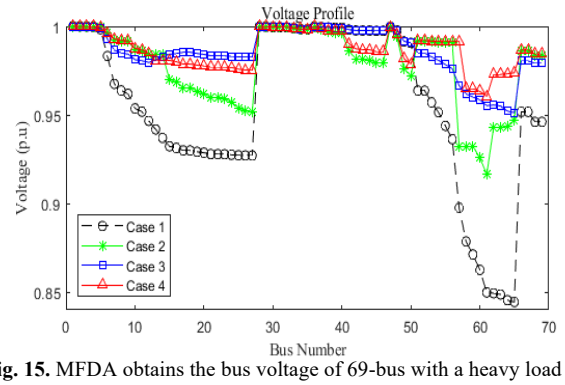

Fig. 15. MFDA obtains the bus voltage of 69-bus with a heavy load in all cases.

Table 17. For a 69-bus with a nominal load, MFDA is compared against other algorithms.

Method	Description	Case 2	Case 3	Case 4
MFDA	Open Switches	14−57−61−69−70	69−70−71−72−73	12−55−62−69−70
	Size in kW (Bus)	-	2090.49	1949.14
	APLRI (%)	56.18	67.06	82.62
	RPLRI (%)	9.9	63.69	64.19
	V_{min} (p.u.)	0.9495 (61)	0.9705 (65)	0. 9806 (61)
ISCA [2]	Open Switches	61−69−14−55−70	69−70−71−72−73	12−19−69−63−57
	Size in kW (Bus)	-	2281.2	1873.1
	APLRI (%)	56.18	66.93	82.34
	RPLRI (%)	9.91	63.85	63.31
	V_{min} (p.u.)	0.9495 (61)	0.9717	0.9798
HSA [46]	Open Switches	69−18−13−56−61	69−70−71−72−73	69−17−13−58−61
	Size in kW (Bus)	-	1773.2	1871.8
	APLRI (%)	55.85	61.43	82.08
	RPLRI (%)	12.08	58.45	64.13
	V_{min} (p.u.)	0.9428	0.9677	0.9736

FWA [3]	Open Switches	69−70−14−56−61	69−70−71−72−73	69−70−13−55−63
	Size in kW (Bus)	-	1832.9	1818.2
	APLRI (%)	56.17	65.39	82.55
	RPLRI (%)	9.91	61.97	63.48
	V_{min} (p.u.)	0.9495	0.9740	0.9796
GA [46]	Open Switches	69−70−14−53, 61	69, 70, 71, 72, 73	10, 15, 45, 55, 62
	Size in kW (Bus)	-	1947.1	2029.2
	APLRI (%)	54.08	60.66	73.38
	RPLRI (%)	-	-	-
	V_{min} (p.u.)	0.9411	0.9687	0.9727
RGA [46]	Open Switches	69−17−13−55−61	69−70−71−72−73	10−16−14−55−62
	Size in kW (Bus)	-	1786.8	2065.4
	APLRI (%)	55.42	61.04	80.32
	RPLRI (%)	-	-	-
	V_{min} (p.u.)	0.9428	0.9678	0.9742

In the same way, the performance of MFDA is compared to that of ISCA [2], HSA [46], and FWA [3] at the heavy loading condition. The outputs are summarized in Table 18 above. In cases 2, 3, and 4, the results indicate that the APLRI% and RPLRI% achieved by the MFDA are significantly superior to those obtained by the ISCA [2], HSA [46], and FWA [3] in cases 2, 3, and 4. Thus, the MFDA achieves better results than other algorithms on all three measures. Figure 13, 14, and 15 displays the voltage profiles of light, nominal, and heavy for all the cases like the base case, light, nominal, and heavy load conditions attained by the proposed MFDA. The convergence curve of the light, nominal, and heavy load conditions are shown in Figures 16 (a), 16 (b), and 16 (c) for the cases.

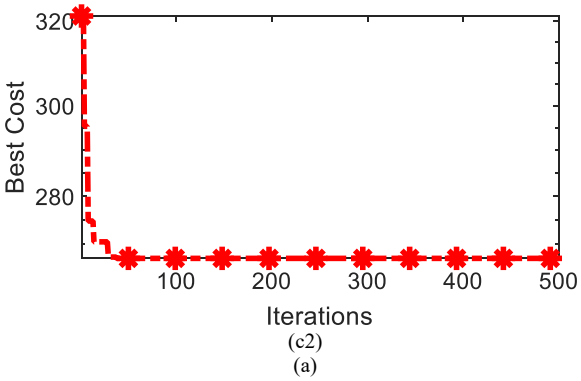

(c2)
(a)

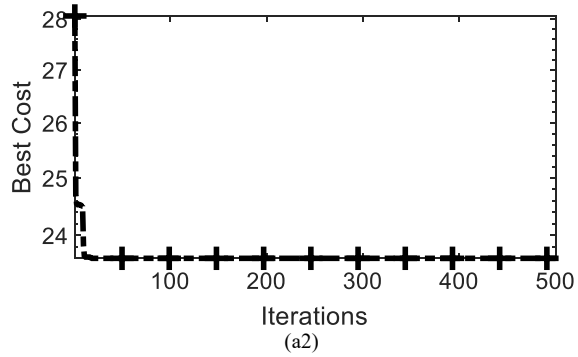

(a2)

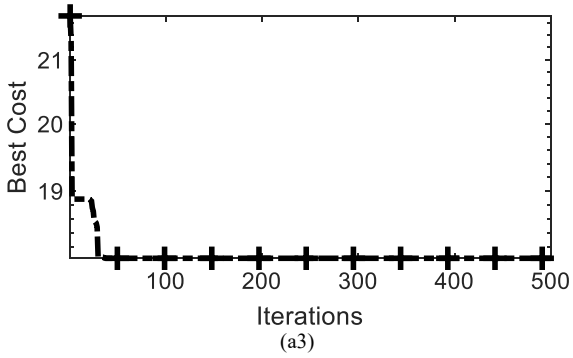

(a3)

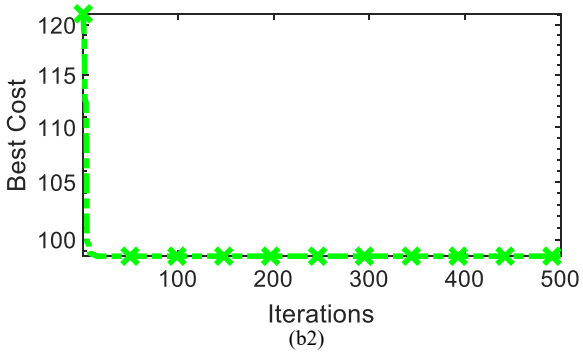

(b2)

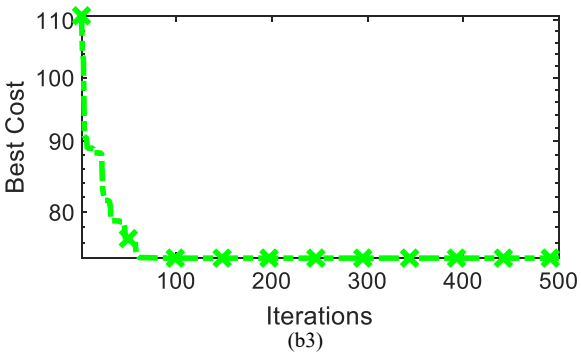

(b3)

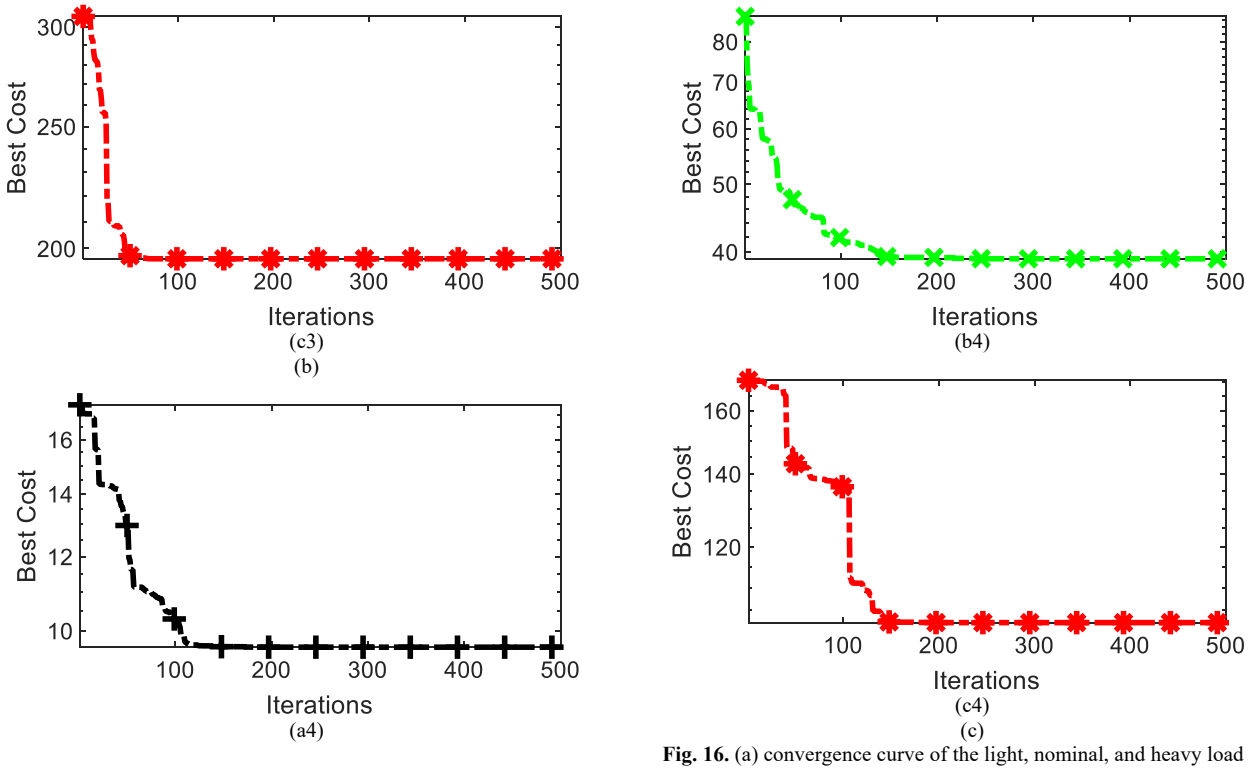

Fig. 16. (a) convergence curve of the light, nominal, and heavy load conditions for case 2, (b) convergence curve of the light, nominal, and heavy load conditions for case 3 and (c) convergence curve of the light, nominal, and heavy load conditions for case 4.

Table 18. For a 69-bus with a heavy load, MFDA is compared against other algorithms.

Method	Description	Case 2	Case 3	Case 4
MFDA	Open Switches	14−56−61−69−70	69−70−71−72−73	12−56−62−69−70
	Size in kW (Bus)	-	3366.07	3142.24
	APLRI (%)	59.06	69.92	84.32
	RPLRI (%)	15.5	66.75	67.49
	V_{min} (p.u.)	0.9165 (61)	0.9513 (65)	0.9687 (61)
ISCA [2]	Open Switches	14−55−61−69−70	69−70−71−72−73	69−70−14−55−62
	Size in kW (Bus)	-	3650.4	2744.9
	APLRI (%)	59.06	69.85	83.99
	RPLRI (%)	15.51	66.93	65.79
	V_{min} (p.u.)	0.9165	0.9530	0.9638
HSA [46]	Open Switches	69−18−13−56−61	69−70−71−72−73	69−18−13−58−61
	Size in kW (Bus)	-	2960.7	3382.8
	APLRI (%)	58.4	64.66	83.96
	RPLRI (%)	17.48	61.82	62.24
	V_{min} (p.u.)	0.9048	0.9478	0.9592
FWA [3]	Open Switches	69−70−14−56−61	69−70−71−72−73	69−70−13−55−63
	Size in kW (Bus)	-	2932.7	2961.3
	APLRI (%)	59.06	68.35	84.21
	RPLRI (%)	15.50	65.09	67.01
	V_{min} (p.u.)	0.9165	0.9568	0.9685

5 Conclusions

This article provides an efficient implementation of MFDA for simultaneous ONR and ODG installation. First, the viability of the recommended technique has been demonstrated by considering six typical sixteen benchmark functions that each have unique features. The power losses were reduced using ONR, ODG, and simultaneous ONR and ODG installation. Among these three ways, simultaneous ONR and ODG installation was better at lowering PL and raising the VP. In the case of simultaneous ONR and ODG installation for nominal loading conditions, the MFDA found the best solution, which reduced power loss by 71.2% for 33 bus systems and 82.62% for 69 bus systems. It improved the minimum voltage to 0.9724 for 33 bus systems and 0.9806 for 69 bus systems. The investigation also showed that the MFDA is the most reliable and efficient technique for simultaneous ONR and ODG installation of both test systems. The optimal solutions found by the MFDA also had a better VP and the lowermost PL than those found by other approaches that have been previously discussed. The MFDA

can be an excellent way to deal with ONR, ODG installation, or simultaneous ONR and ODG installation.

This is an Open Access article distributed under the terms of the Creative Commons Attribution License.

References

[1] T. T. Nguyen, A. V. Truong, and T. A. Phung, "A novel method based on adaptive cuckoo search for optimal network reconfiguration and distributed generation allocation in distribution network," *Int. J. Electr. Pow. Ener. Sys.*, vol. 78, pp. 801–815, Jun. 2016, doi: 10.1016/J.IJEPES.2015.12.030.

[2] U. Raut and S. Mishra, "An improved sine–cosine algorithm for simultaneous network reconfiguration and DG allocation in power distribution systems," *Appl. Soft Comp. J.*, vol. 92, Jul. 2020, doi: 10.1016/j.asoc.2020.106293.

[3] A. M. Imran, M. Kowsalya, and D. P. Kothari, "A novel integration technique for optimal network reconfiguration and distributed generation placement in power distribution networks," *Int. J. Electr. Pow. Ener. Sys.*, vol. 63, pp. 461–472, Dec. 2014, doi: 10.1016/J.IJEPES.2014.06.011.

[4] B. Wang and H. Z. Cheng, "Optimization of network configuration in large distribution systems using plant growth simulation algorithm," *IEEE Transac. Pow. Sys*., vol. 23, no. 1, pp. 119–126, Feb. 2008, doi: 10.1109/TPWRS.2007.913293.

[5] Y. Abdelaziz, F. M. Mohammed, S. F. Mekhamer, and M. A. L. Badr, "Distribution Systems Reconfiguration using a modified particle swarm optimization algorithm," *Elect. Pow. Sys. Res.*, vol. 79, no. 11, pp. 1521–1530, Nov. 2009, doi: 10.1016/j.epsr.2009.05.004.

[6] Y. K. Wu, C. Y. Lee, L. C. Liu, and S. H. Tsai, "Study of reconfiguration for the distribution system with distributed generators," *IEEE Trans. Pow. Deliv.*, vol. 25, no. 3, pp. 1678–1685, Jul. 2010, doi: 10.1109/TPWRD.2010.2046339.

[7] R. Srinivasa Rao, S. V. L. Narasimham, M. Ramalinga Raju, and A. Srinivasa Rao, "Optimal network reconfiguration of large-scale distribution system using harmony search algorithm," *IEEE Transac. Pow. Sys.,* vol. 26, no. 3, pp. 1080–1088, Aug. 2011, doi: 10.1109/TPWRS.2010.2076839.

[8] A. Y. Abdelaziz, R. A. Osama, and S. M. Elkhodary, "Distribution systems reconfiguration using ant colony optimization and harmony search algorithms," *Elect. Pow. Compon. Sys.,* vol. 41, no. 5, pp. 537–554, May 2013, doi: 10.1080/15325008.2012.755232.

[9] J. A. Martín García and A. J. Gil Mena, "Optimal distributed generation location and size using a modified teaching-learning based optimization algorithm," *Int. J. Elect. Pow. Ener. Sys.,* vol. 50, no. 1, pp. 65–75, Sep. 2013, doi: 10.1016/j.ijepes.2013.02.023.

[10] J. Torres, J. L. Guardado, F. Rivas-Dávalos, S. Maximov, and E. Melgoza, "A genetic algorithm based on the edge window decoder technique to optimize power distribution systems reconfiguration," *Int. J. Elect. Pow. Ener. Sys.,* vol. 45, no. 1, pp. 28–34, Feb. 2013, doi: 10.1016/j.ijepes.2012.08.075.

[11] Y. Lakshmi Reddy, T. Sathiyanarayanan, and M. Sydulu, "Application of firefly algorithm for radial distribution network reconfiguration using different loads," in *IFAC Proceed. Volum. (IFAC-PapersOnline)*, IFAC Secretariat, Mar. 2014, pp. 700–705. doi: 10.3182/20140313-3-IN-3024.00052.

[12] E. Azad-Farsani, M. Zare, R. Azizipanah-Abarghooee, and H. Askarian-Abyaneh, "A new hybrid CPSO-TLBO optimization algorithm for distribution network reconfiguration," *J. Intell. Fuzzy Sys.* , vol. 26, no. 5, pp. 2175–2184, Oct. 2014, doi: 10.3233/IFS-130892.

[13] S. Teimourzadeh and K. Zare, "Application of binary group search optimization to distribution network reconfiguration," *Int. J. Elect. Pow. Ener. Sys.,* vol. 62, pp. 461–468, Nov. 2014, doi: 10.1016/j.ijepes.2014.04.064.

[14] R. Sedaghati, M. Hakimzadeh, H. Fotoohabadi, and A. R. Rajabi, "Study of network reconfiguration in distribution systems using an Adaptive Modified Firefly Algorithm," *Automatika*, vol. 57, no. 1, pp. 27–36, Jan. 2016, doi: 10.7305/automatika.2016.07.858.

[15] M. Abdelaziz, "Distribution network reconfiguration using a genetic algorithm with varying population size," *Elect. Pow. Sys. Res.*, vol. 142, pp. 9–11, Jan. 2017, doi: 10.1016/j.epsr.2016.08.026.

[16] R. Pegado, Z. Ñaupari, Y. Molina, and C. Castillo, "Radial distribution network reconfiguration for power losses reduction based on improved selective BPSO," *Elec. Power Sys. Res.*, vol. 169, pp. 206–213, Apr. 2019, doi: 10.1016/j.epsr.2018.12.030.

[17] T. Tran The, D. Vo Ngoc, and N. Tran Anh, "Distribution Network Reconfiguration for Power Loss Reduction and Voltage Profile Improvement Using Chaotic Stochastic Fractal Search Algorithm," *Complexity*, vol. 2020, Mar. 2020, doi: 10.1155/2020/2353901.

[18] T. T. Nguyen, Q. T. Nguyen, and T. T. Nguyen, "Optimal radial topology of electric unbalanced and balanced distribution system using improved coyote optimization algorithm for power loss reduction," *Neural Comput Appl*, vol. 33, no. 18, pp. 12209–12236, Sep. 2021, doi: 10.1007/s00521-021-06175-4.

[19] H. Hizarci, O. Demirel, and B. E. Turkay, "Distribution network reconfiguration using time-varying acceleration coefficient assisted binary particle swarm optimization," *Eng. Sci. Techn. Int. J.*, vol. 35, Nov. 2022, doi: 10.1016/j.jestch.2022.101230.

[20] M. Cikan and B. Kekezoglu, "Comparison of metaheuristic optimization techniques including Equilibrium optimizer algorithm in power distribution network reconfiguration," *Alexandria Eng. J.*, vol. 61, no. 2, pp. 991–1031, Feb. 2022, doi: 10.1016/j.aej.2021.06.079.

[21] Y. J. Jeon, J. C. Kim, J. O. Kim, J. R. Shin, and K. Y. Lee, "An efficient simulated annealing algorithm for network reconfiguration in large-scale distribution systems," *IEEE Trans. Pow. Deliv.*, vol. 17, no. 4, pp. 1070–1078, Oct. 2002, doi: 10.1109/TPWRD.2002.803823.

[22] E. Haesen, J. Driesen, and R. Belmans, "Robust planning methodology for integration of stochastic generators in distribution grids," *IET Renew. Pow. Gener*, vol. 1, no. 1, pp. 25–32, Mar. 2007, doi: 10.1049/iet-rpg:20060012.

[23] M. R. Alrashidi and M. F. Alhajri, "Optimal planning of multiple distributed generation sources in distribution networks: A new approach," *Ener. Convers. Manag.*, vol. 52, no. 11, pp. 3301–3308, Oct. 2011, doi: 10.1016/j.enconman.2011.06.001.

[24] F. S. Abu-Mouti and M. E. El-Hawary, "Optimal distributed generation allocation and sizing in distribution systems via artificial bee colony algorithm," *IEEE Trans. Pow. Deliv.*, vol. 26, no. 4, pp. 2090–2101, Oct. 2011, doi: 10.1109/TPWRD.2011.2158246.

[25] M. H. Moradi and M. Abedini, "A combination of genetic algorithm and particle swarm optimization for optimal DG location and sizing in distribution systems," *Int. J. Elect. Pow. Ener. Sys.,*vol. 34, no. 1, pp. 66–74, Jan. 2012, doi: 10.1016/j.ijepes.2011.08.023.

[26] H. Doagou-Mojarrad, G. B. Gharehpetian, H. Rastegar, and J. Olamaei, "Optimal placement and sizing of DG (distributed generation) units in distribution networks by novel hybrid evolutionary algorithm," *Energy*, vol. 54, pp. 129–138, Jun. 2013, doi: 10.1016/j.energy.2013.01.043.

[27] M. M. Aman, G. B. Jasmon, A. H. A. Bakar, and H. Mokhlis, "A new approach for optimum DG placement and sizing based on voltage stability maximization and minimization of power losses," *Energy Convers Manag*, vol. 70, pp. 202–210, Jun. 2013, doi: 10.1016/j.enconman.2013.02.015.

[28] M. M. Aman, G. B. Jasmon, A. H. A. Bakar, and H. Mokhlis, "A new approach for optimum simultaneous multi-DG distributed generation Units placement and sizing based on maximization of system loadability using HPSO (hybrid particle swarm optimization) algorithm," *Energy*, vol. 66, pp. 202–215, Mar. 2014, doi: 10.1016/j.energy.2013.12.037.

[29] A. El-Fergany, "Study impact of various load models on DG placement and sizing using backtracking search algorithm," *Appl. Soft Comp. J.*, vol. 30, pp. 803–811, May 2015, doi: 10.1016/j.asoc.2015.02.028.

[30] N. Kanwar, N. Gupta, K. R. Niazi, and A. Swarnkar, "Simultaneous allocation of distributed resources using improved teaching learning based optimization," *Ener. Conv. Manag*, vol. 103, pp. 387–400, Oct. 2015, doi: 10.1016/J.ENCONMAN.2015.06.057.

[31] D. Rama Prabha and T. Jayabarathi, "Optimal placement and sizing of multiple distributed generating units in distribution networks by invasive weed optimization algorithm," *Ain Shams Eng. J.*, vol. 7, no. 2, pp. 683–694, Jun. 2016, doi: 10.1016/j.asej.2015.05.014.

[32] E. S. Oda, A. A. Abdelsalam, M. N. Abdel-Wahab, and M. M. El-Saadawi, "Distributed generations planning using flower pollination algorithm for enhancing distribution system voltage stability," *Ain*

Shams Eng, J., vol. 8, no. 4, pp. 593–603, Dec. 2017, doi: 10.1016/j.asej.2015.12.001.

[33] S. A. ChithraDevi, L. Lakshminarasimman, and R. Balamurugan, "Stud Krill herd Algorithm for multiple DG placement and sizing in a radial distribution system," *Engineer. Sci. Techn. Int. J.,* vol. 20, no. 2, pp. 748–759, Apr. 2017, doi: 10.1016/j.jestch.2016.11.009.

[34] U. Sultana, A. B. Khairuddin, A. S. Mokhtar, N. Zareen, and B. Sultana, "Grey wolf optimizer based placement and sizing of multiple distributed generation in the distribution system," *Energy*, vol. 111, pp. 525–536, Sep. 2016, doi: 10.1016/j.energy.2016.05.128.

[35] H. Hamour, S. Kamel, H. Abdel-Mawgoud, A. Korashy, and F. Jurado, "Distribution network reconfiguration using grasshopper optimization algorithm for power loss minimization," *2018 Int. Conf. Smart Ener. Sys. Techn., SEST 2018 - Proc.*, Oct. 2018, doi: 10.1109/SEST.2018.8495659.

[36] D. B. Prakash and C. Lakshminarayana, "Multiple DG placements in radial distribution system for multi objectives using Whale Optimization Algorithm," *Alexandria Eng. J.*, vol. 57, no. 4, pp. 2797–2806, Dec. 2018, doi: 10.1016/j.aej.2017.11.003.

[37] S. Kamel, A. Awad, H. Abdel-Mawgoud, and F. Jurado, "Optimal DG allocation for enhancing voltage stability and minimizing power loss using hybrid gray Wolf optimizer," *Turkish J. Electr. Eng. Comp. Sci.,* vol. 27, no. 4, pp. 2947–2961, Jan. 2019, doi: 10.3906/elk-1805-66.

[38] J. Radosavljevic, N. Arsic, M. Milovanovic, and A. Ktena, "Optimal Placement and Sizing of Renewable Distributed Generation Using Hybrid Metaheuristic Algorithm," *J. Modern Pow. Sys. Clean Ener.,* vol. 8, no. 3, pp. 499–510, May 2020, doi: 10.35833/MPCE.2019.000259.

[39] G. Deb, K. Chakraborty, and S. Deb, "Modified Spider Monkey Optimization-Based Optimal Placement of Distributed Generators in Radial Distribution System for Voltage Security Improvement," *Elect. Pow. Compon. Sys.,* vol. 48, no. 9–10, pp. 1006–1020, Oct. 2020, doi: 10.1080/15325008.2020.1829186.

[40] A. Selim, S. Kamel, A. S. Alghamdi, and F. Jurado, "Optimal Placement of DGs in Distribution System Using an Improved Harris Hawks Optimizer Based on Single- and Multi-Objective Approaches," *IEEE Access*, vol. 8, pp. 52815–52829, Mar. 2020, doi: 10.1109/ACCESS.2020.2980245.

[41] K. H. Truong, P. Nallagownden, I. Elamvazuthi, and D. N. Vo, "A Quasi-Oppositional-Chaotic Symbiotic Organisms Search algorithm for optimal allocation of DG in radial distribution networks," *Appl. Soft Comp. J.*, vol. 88, Mar. 2020, doi: 10.1016/j.asoc.2020.106067.

[42] Z. Tan, M. Zeng, and L. Sun, "Optimal Placement and Sizing of Distributed Generators Based on Swarm Moth Flame Optimization," *Front Ener. Res.*, vol. 9, Apr. 2021, doi: 10.3389/fenrg.2021.676305.

[43] M. G. Hemeida, A. A. Ibrahim, A. A. A. Mohamed, S. Alkhalaf, and A. M. B. El-Dine, "Optimal allocation of distributed generators DG based Manta Ray Foraging Optimization algorithm (MRFO)," *Ain Shams Eng. J.*, vol. 12, no. 1, pp. 609–619, Mar. 2021, doi: 10.1016/j.asej.2020.07.009.

[44] K. S. Sambaiah and T. Jayabarathi, "Optimal reconfiguration and renewable distributed generation allocation in electric distribution systems," *Int. J. Ambient Ener.*, vol. 42, no. 9, pp. 1018–1031, 2021, doi: 10.1080/01430750.2019.1583604.

[45] R. S. Rao, K. Ravindra, K. Satish, and S. V. L. Narasimham, "Power loss minimization in distribution system using network reconfiguration in the presence of distributed generation," *IEEE Transac. Pow. Sys.*, vol. 28, no. 1, pp. 317–325, 2013, doi: 10.1109/TPWRS.2012.2197227.

[46] S. H. Mirhoseini, S. M. Hosseini, M. Ghanbari, and M. Ahmadi, "A new improved adaptive imperialist competitive algorithm to solve the reconfiguration problem of distribution systems for loss reduction and voltage profile improvement," *Int. J. Elect. Pow. Ener. Sys.,* vol. 55, pp. 128–143, 2014, doi: 10.1016/j.ijepes.2013.08.028.

[47] S. R. Tuladhar, J. G. Singh, and W. Ongsakul, "Multi-objective approach for distribution network reconfiguration with optimal DG power factor using NSPSO," *IET Gener., Transm. Distrib.*, vol. 10, no. 12, pp. 2842–2851, Sep. 2016, doi: 10.1049/iet-gtd.2015.0587.

[48] A. Bayat, A. Bagheri, and R. Noroozian, "Optimal siting and sizing of distributed generation accompanied by reconfiguration of distribution networks for maximum loss reduction by using a new UVDA-based heuristic method," *Int. J. Elect. Pow. Ener. Sys.,* vol. 77, pp. 360–371, May 2016, doi: 10.1016/j.ijepes.2015.11.039.

[49] M. Abd El-salam, E. Beshr, and M. Eteiba, "A New Hybrid Technique for Minimizing Power Losses in a Distribution System by Optimal Sizing and Siting of Distributed Generators with Network Reconfiguration," *Energies (Basel)*, vol. 11, no. 12, p. 3351, Nov. 2018, doi: 10.3390/en11123351.

[50] J. Siahbalaee, N. Rezanejad, and G. B. Gharehpetian, "Reconfiguration and DG Sizing and Placement Using Improved Shuffled Frog Leaping Algorithm," *Elect. Pow. Compon. Sys.,* vol. 47, no. 16–17, pp. 1475–1488, Oct. 2019, doi: 10.1080/15325008.2019.1689449.

[51] A. Onlam, D. Yodphet, R. Chatthaworn, C. Surawanitkun, A. Siritaratiwat, and P. Khunkitti, "Power loss minimization and voltage stability improvement in electrical distribution system via network reconfiguration and distributed generation placement using novel adaptive shuffled frogs leaping algorithm," *Energies (Basel)*, vol. 12, no. 3, Art. no. 553, Feb. 2019, doi: 10.3390/en12030553.

[52] U. Raut and S. Mishra, "An improved Elitist–Jaya algorithm for simultaneous network reconfiguration and DG allocation in power distribution systems," *Renew. Ener. Focus*, vol. 30, pp. 92–106, Sep. 2019, doi: 10.1016/j.ref.2019.04.001.

[53] A. Quadri and S. Bhowmick, "A hybrid technique for simultaneous network reconfiguration and optimal placement of distributed generation resources," *Soft Comp.*, vol. 24, no. 15, pp. 11315–11336, Aug. 2020, doi: 10.1007/s00500-019-04597-w.

[54] T. T. The, S. N. Quoc, and D. V. Ngoc, "Symbiotic Organism Search Algorithm for Power Loss Minimization in Radial Distribution Systems by Network Reconfiguration and Distributed Generation Placement," *Math Probl. Eng.*, vol. 2020, Art. no. 1615792, Jun. 2020, doi: 10.1155/2020/1615792.

[55] H. Teimourzadeh and B. Mohammadi-Ivatloo, "A three-dimensional group search optimization approach for simultaneous planning of distributed generation units and distribution network reconfiguration," *Appl. Soft Comput.*, vol. 88, Art no. 106012, Mar. 2020, doi: 10.1016/j.asoc.2019.106012.

[56] T. T. Tran, K. H. Truong, and D. N. Vo, "Stochastic fractal search algorithm for reconfiguration of distribution networks with distributed generations," *Ain Shams Eng. J.*, vol. 11, no. 2, pp. 389–407, Jun. 2020, doi: 10.1016/j.asej.2019.08.015.

[57] U. Raut and S. Mishra, "Enhanced Sine–Cosine Algorithm for Optimal Planning of Distribution Network by Incorporating Network Reconfiguration and Distributed Generation," *Arab J. Sci. Eng.*, vol. 46, no. 2, pp. 1029–1051, Feb. 2021, doi: 10.1007/s13369-020-04808-9.

[58] T. T. Nguyen, T. T. Nguyen, L. T. Duong, and V. A. Truong, "An effective method to solve the problem of electric distribution network reconfiguration considering distributed generations for energy loss reduction," *Neural Comput. Appl.*, vol. 33, no. 5, pp. 1625–1641, Mar. 2021, doi: 10.1007/s00521-020-05092-2.

[59] A. M. Shaheen, A. M. Elsayed, R. A. El-Sehiemy, and A. Y. Abdelaziz, "Equilibrium optimization algorithm for network reconfiguration and distributed generation allocation in power systems," *Appl. Soft Comput.*, vol. 98, Art no. 106867, Jan. 2021, doi: 10.1016/j.asoc.2020.106867.

[60] T. Van Tran, B. H. Truong, T. P. Nguyen, T. A. Nguyen, T. L. Duong, and D. N. Vo, "Reconfiguration of Distribution Networks with Distributed Generations Using an Improved Neural Network Algorithm," *IEEE Access*, vol. 9, pp. 165618–165647, Dec. 2021, doi: 10.1109/ACCESS.2021.3134872.

[61] M. T. Nguyen Hoang, B. H. Truong, K. T. Hoang, K. Dang Tuan, and D. Vo Ngoc, "A Quasioppositional-Chaotic Symbiotic Organisms Search Algorithm for Distribution Network Reconfiguration with Distributed Generations," *Math Probl. Eng.*, vol. 2021, Art no. 2065043, Dec. 2021, doi: 10.1155/2021/2065043.

[62] T. T. Nguyen, T. L. Duong, and T. Q. Ngo, "Network Reconfiguration and Distributed Generation Placement for Multi-Goal Function Based on Improved Moth Swarm Algorithm," *Math Probl. Eng.*, vol. 2022, Art no. 5015771, Apr. 2022, doi: 10.1155/2022/5015771.

[63] M. Ntombela, K. Musasa, and M. C. Leoaneka, "Power Loss Minimization and Voltage Profile Improvement by System Reconfiguration, DG Sizing, and Placement," *Computation*, vol. 10, no. 10, pp 1- 22, Oct. 2022, doi: 10.3390/computation10100180.

[64] A. M. Shaheen, A. M. Elsayed, R. A. El-Sehiemy, S. Kamel, and S. S. M. Ghoneim, "A modified marine predators optimization algorithm for simultaneous network reconfiguration and distributed generator allocation in distribution systems under different loading conditions," *Eng. Optimiz.*, vol. 54, no. 4, pp. 687–708, Apr. 2022, doi: 10.1080/0305215X.2021.1897799.

[65] P. P. Biswas, R. Mallipeddi, P. N. Suganthan, and G. A. J. Amaratunga, "A multiobjective approach for optimal placement and sizing of distributed generators and capacitors in distribution

network," *Appl. Soft Comp. J.*, vol. 60, pp. 268–280, Nov. 2017, doi: 10.1016/j.asoc.2017.07.004.

[66] H. Karami, M. V. Anaraki, S. Farzin, and S. Mirjalili, "Flow Direction Algorithm (FDA): A Novel Optimization Approach for Solving Optimization Problems," *Comput. Ind. Eng.*, vol. 156, Art. no. 107224, Jun. 2021, doi: 10.1016/j.cie.2021.107224.

[67] O. Badran, H. Mokhlis, S. Mekhilef, W. Dahalan, and J. Jallad, "Minimum switching losses for solving distribution NR problem with distributed generation," *IET Gener. Transm. Distrib.*, vol. 12, no. 8, pp. 1790–1801, Apr. 2018, doi: 10.1049/iet-gtd.2017.0595.

[68] R. D. Zimmerman, C. E. Murillo-Sánchez, and R. J. Thomas, "MATPOWER: Steady-state operations, planning, and analysis tools for power systems research and education," *IEEE Transac. Pow. Sys.,* vol. 26, no. 1, pp. 12–19, Feb. 2011, doi: 10.1109/TPWRS.2010.2051168.

[69] M. E. Baran and F. F. Wu, "Network reconfiguration in distribution systems for loss reduction and load balancing," *IEEE Trans. Pow. Deliv.*, vol. 4, no. 2, pp. 1401–1407, 1989, doi: 10.1109/61.25627.

[70] R. Panda, M. Swain, M. K. Naik, S. Agrawal, and A. Abraham, "A Novel Practical Decisive Row-Class Entropy-Based Technique for Multilevel Threshold Selection Using Opposition Flow Directional Algorithm," *IEEE Access*, vol. 10, pp. 110473–110484, Oct. 2022, doi: 10.1109/ACCESS.2022.3215082.